Copyright © 2012 Tech Science Press CMES, vol.85, no.1, pp.1-43, 2012

# A Simple Multi-Source-Point Trefftz Method for Solving Direct/Inverse SHM Problems of Plane Elasticity in Arbitrary Multiply-Connected Domains

**L. Dong**[1] **and S. N. Atluri**[1]

**Abstract:** In this paper, a generalized Trefftz method in plane elasticity is developed, for solving problems in an arbitrary multiply connected domain. Firstly, the relations between Trefftz basis functions from different source points are discussed, by using the binomial theorem and the logarithmic binomial theorem. Based on these theorems, we clearly explain the relation between the T-Trefftz and the F-Trefftz methods, and why the traditional T-Trefftz method, which uses only one source point, cannot successfully solve problems in a multiply connected domain with genus larger than 1. Thereafter, a generalized Trefftz method is proposed, which uses logarithmic and negative power series from multiple source points, and positive power series from only one source point, as complex potentials. In addition, a characteristic length for each source point is used to scale the Trefftz basis functions, in order to resolve the ill-posedness of Trefftz methods. For direct problems, no further regularization techniques are used, because the coefficient matrix of the system of linear equations to be solved is already well-conditioned, by using characteristic lengths to scale the Trefftz basis functions. Inverse problems in plane elasticity, wherein both tractions as well as displacements, or, both strains as well as displacements, are prescribed at a part of the boundary, and the data at the other part of the boundary and in the domain have to be solved for, are also considered. These problems are of importance in Structural Health Monitoring (SHM). For inverse problems where noises are present, a very simple regularization method is used, to mitigate the inherent ill-posed nature of inverse problems. By several numerical examples, we show that this generalized Trefftz method can successfully solve both direct/inverse problems in simply as well as multiply connected domains. Therefore, we consider this multi-source-point multi-characteristic-length-scale Trefftz method to be simple, general as well as very useful. And the essential idea of how to construct basis functions from multiple source points can be used to develop other Trefftz methods, as well as special Trefftz Voronoi Cell Finite Elements, with

[1] Center for Aerospace Research & Education, University of California, Irvine

circular, elliptical, or arbitrary shaped voids and rigid/flexible inclusions.

**Keywords:** T-Trefftz, F-Trefftz, elasticity, multiply connected domain, binomial theorem, characteristic length, ill-posed

## 1 Introduction

Since being introduced by [Trefftz (1926)], Trefftz methods have shown their accuracy and efficiency in solving various physical/mathematical problems, including: Poisson equation, Laplace equation, Helmholtz equation, biharmonic equation, elasticity problems, plate bending problems, free vibration problems, eigenvalue problems, etc, see [Cheung, Jin and Zienkiewicz (1989, 1990, 1991, 1993); Kamiya and Wu (1994); Kita, Kamiya and Iio (1999); Chang, Liu, Kuo and Yeih (2003); Li, Lu, Tsai and Cheng (2006); Liu (2007a, 2007b); Liu, Yeih and Atluri (2009); Yeih, Liu, Kuo and Atluri (2010)]. Among these methods, T-Trefftz methods use the so-called T-complete functions from one source point, which satisfy the governing differential equations a priori, as trial or test functions. On the other hand, F-Trefftz methods use fundamental solutions from multiple source points as trial or test functions. In addition, when Trefftz basis functions are used to construct trial functions, it is called the indirect Trefftz method. If Trefftz basis functions are used to construct test functions, it is often referred to as the direct Trefftz method. Trefftz methods were combined with the Finite Element Method (FEM) to develop hybrid Trefftz FEM for elasticity problems [Jirousek and Teodorescu (1982)], plate bending problems [Jirousek and Guex (1986)], as well as Trefftz Voronoi Cell Finite Elements (Trefftz VCFEMs) to model micromechanical behaviors of heterogeneous materials [Dong and Atluri (2011); Dong and Atluri (2012)]. A useful review of various Trefftz methods can be found in [Kita and Kamiya (1995)]. In this study, only the indirect Trefftz method is considered.

Despite of the high performances of Trefftz methods, there are two major drawbacks. As described in [Yeih, Liu, Kuo and Atluri (2010)], one is how to solve a ill-posed system of equations that is generated by Trefftz methods, and the other one is the inconvenience of Trefftz methods in tackling problems in multiply connected domains. For Laplace equations, [Liu (2007a, 2007b)] introduced the concept of scaling Trefftz basis functions by characteristic lengths, which successfully resolved the ill-posedness of Trefftz methods, and this was extended to solve general ill-conditioned linear algebra equations in [Liu, Yeih and Atluri (2009)]. On the other hand, based on detailed discussion of Trefftz basis functions from various source points, an approach of constructing multiple-source-point Trefftz basis functions were developed in [Yeih, Liu, Kuo and Atluri (2010)]. This generalized Trefftz method can be used to solve Laplace equations in arbitrarily multiply connected domain. However, for other important problems such as linear elastic solid mechanics, detailed investigations of Trefftz basis functions from various source points remain necessary, in order to construct a complete set of basis functions for arbitrarily multiply connected domain.

In this study, following the work of [Yeih, Liu, Kuo and Atluri (2010)], we develop a generalized Trefftz method in linear elasticity. We start in section 2 by discussing the relation between Trefftz basis functions from different source points, using binomial theorem and logarithmic binomial theorem. Some comments are thereafter obtained on how to construct a complete set of Trefftz basis functions. Based on these comments, a multi-source-point Trefftz method is developed in section 3, and a characteristic length is used for each source point to scale the Trefftz basis functions. A simple regularization method is also used to resolve the ill-posedness of inverse Cauchy problems. By several numerical examples in section 4, we demonstrate that this generalized Trefftz method can solve not only forward but also ill-posed inverse problems in multiply, and of course simply connected domains. Therefore, we consider this unified approach simple, general, and very useful, and thus recommend for engineering applications. In section 5, we complete this paper by some concluding remarks.

## 2 Trefftz Basis Functions from Different Source Points

Consider a linear elastic solid undergoing infinitesimal elasto-static deformation. Cartesian coordinates $x_i$ identify material particles in the solid. $\sigma_{ij}, \varepsilon_{ij}, u_i$ are Cartesian components of the stress tensor, strain tensor and displacement vector respectively. $\overline{f_i}$ are Cartesian components of the prescribed body force. We use $()_{,i}$ to denote differentiation with respect to $x_i$. The equations of linear and angular momentum balance, constitutive equations, and compatibility equations can be written as:

$$\sigma_{ij,j} + \overline{f}_i = 0 \text{ in } \Omega \tag{1}$$

$$\sigma_{ij} = \sigma_{ji} \text{ in } \Omega \tag{2}$$

$$\sigma_{ij} = C_{ijkl}\varepsilon_{kl} \text{ (or } \varepsilon_{ij}{=}S_{ijkl}\sigma_{kl}) \text{ in } \Omega \text{ for a linear elastic solid} \tag{3}$$

$$\varepsilon_{ij} = \frac{1}{2}\left(u_{i,j} + u_{j,i}\right) \equiv u_{(i,j)} \text{ in } \Omega \tag{4}$$

For isotropic plane elasticity where body force is negligible, equation (1)-(4) can be rewritten in terms of displacements, which is the 2D Navier's equation:

$$(\lambda^* + \mu)\theta_{,i} + \mu\Delta u_i = 0,\ i = 1,2 \tag{5}$$

where

$$\begin{aligned}
&\theta = u_{1,1} + u_{2,2} \\
&\lambda^* = \begin{cases} \frac{2\lambda\mu}{\lambda+2\mu} & \text{for plane stress problems} \\ \lambda & \text{for plane strain problems} \end{cases} \\
&\lambda = \frac{Ev}{(1+v)(1-2v)} \\
&\mu = G = \frac{E}{2(1+v)}
\end{aligned} \tag{6}$$

The T-Trefftz methods start by selecting a set of trial functions which satisfy (5). For isotropic plane stress or plane strain problems where body force are negligible, the basis functions from a source point $S_o : (x_1^o, x_2^o)$ can be generated by two complex potentials $\phi_o(z_o)$ and $\chi_o(z_o)$, see [Muskhelishvili (1954)]:

$$\begin{aligned}
u_1^o + iu_2^o &= \left[\kappa\phi_o(z_o) - z_o\overline{\phi_o'(z_o)} - \overline{\chi_o'(z_o)}\right]/2G \\
\sigma_{11}^o + i\sigma_{12}^o &= \phi_o'(z_o) + \overline{\phi_o'(z_o)} - z_o\overline{\phi_o''(z_o)} - \overline{\chi_o''(z_o)} \\
\sigma_{22}^o - i\sigma_{12}^o &= \phi_o'(z_o) + \overline{\phi_o'(z_o)} + z_o\overline{\phi_o''(z_o)} + \overline{\chi_o''(z_o)}
\end{aligned} \tag{7}$$

In (7), $z_o = (x_1 - x_1^o) + i(x_2 - x_2^o)$ with $i = \sqrt{-1}$. $Re[]$ and $Im[]$denote the real and imaginary part of a complex variable. $G$ and $\kappa$ are defined as:

$$\begin{aligned}
&\kappa = \begin{cases} 3-4v & \text{for plane strain problems} \\ (3-v)/(1+v) & \text{for plane stress problems} \end{cases} \\
&G = \frac{E}{2(1+v)}
\end{aligned} \tag{8}$$

where $E, v$ are the Young's modulus and Poisson ratio respectively.

It should be noted that, $\phi_o(z_o)$ and $\chi_o'(z_o)$needs to be selected in such a way that the constructed basis functions are relatively complete for the specific domain of interest. For this reason, the T-Trefftz basis functions are often called T-complete functions. As discussed in [Jin, Cheung and Ziekiewicz (1990)], for a simply connected domain in Fig. 1(a), one locates the source point inside $\Omega$, and assume $\phi_o(z_o)$ and $\chi_o'(z_o)$ in terms of positive power series:

$$\begin{aligned}
\phi_o(z_o) &= \sum_{n=1}^{\infty} \left(i\alpha_n^1 + \alpha_n^2\right) z_o^n \\
\chi_o'(z_o) &= \sum_{n=0}^{\infty} \left(i\alpha_n^3 + \alpha_n^4\right) z_o^n
\end{aligned} \tag{9}$$

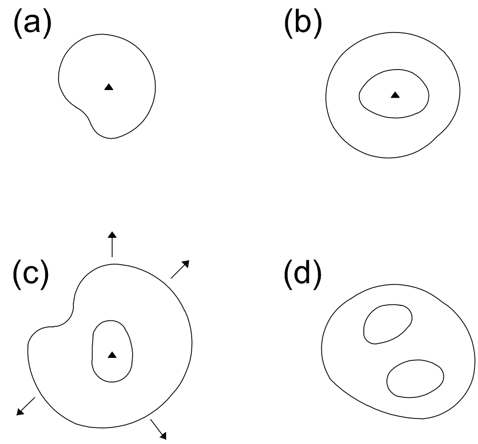


Figure 1: The location of the source point for T-Trefftz methods in (a) a simply connected domain, (b) a finite doubly connected domain, (c) an infinite domain with a cavity, (d) multiply connected domain with genus larger than one

For a doubly connected domain as in Fig. 1(b), one locates the source point inside the cavity, and $\phi_o(z_o)$ and $\chi_o'(z_o)$ are assumed in terms of both positive and negative power series, as well as a logarithmic function:

$$\begin{aligned}\phi_o(z_o) &= (iA+B)\ln z_o + \sum_{n=1}^{\infty}\left(i\alpha_n^1+\alpha_n^2\right)z_o^n + \sum_{n=-1}^{-\infty}\left(i\alpha_n^1+\alpha_n^2\right)z_o^n \\ \chi_o'(z_o) &= \kappa\,(iA-B)\ln z_o + \sum_{n=0}^{\infty}\left(i\alpha_n^3+\alpha_n^4\right)z_o^n + \sum_{n=-1}^{-\infty}\left(i\alpha_n^3+\alpha_n^4\right)z_o^n\end{aligned} \tag{10}$$

For an infinite domain with a cavity as in Fig. 1(c), one locates the source point inside the cavity, and use:

$$\begin{aligned}\phi_o(z_o) &= (iA+B)\ln z_o + \left(i\alpha_1^1+\alpha_1^2\right)z_o + \sum_{n=-1}^{-\infty}\left(i\alpha_n^1+\alpha_n^2\right)z_o^n \\ \chi_o'(z_o) &= \kappa\,(iA-B)\ln z_o + \left(i\alpha_1^3+\alpha_1^4\right)z_o + \sum_{n=0}^{-\infty}\left(i\alpha_n^3+\alpha_n^4\right)z_o^n\end{aligned} \tag{11}$$

However, for a multiply connected domain with genus larger than 1, as seen in Fig. 1(d), it is generally found that the performance of T-Trefftz methods, which only use one source point, is very poor. Other techniques such as domain decomposition has to be used, see [Kita, Kamiya, and Iio (1999)].

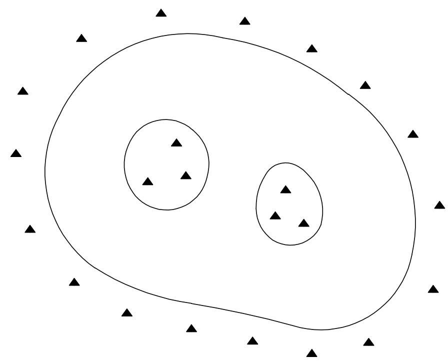

Figure 2: The location of source points for F-Trefftz methods

On the other hand, the F-Trefftz methods, or the so-called method of fundamental solutions, can be used to solve problems in multiply connected domains with genus larger than 1. The F-Trefftz methods use multiple source points outside the domain of interest,$S_l : (x_1^l, x_2^l), l = 1,2,3...$, but only use the fundamental solutions at each source point, as the basis functions, see Fig. 2. The completeness of using fundamental solutions from multiple source points as trial functions has been well established. And the fundamental solutions from a source point can be clearly expressed in terms of complex potentials:

$$\begin{aligned}
\phi_l(z_l) &= -\frac{(F_1 + iF_2)}{2\pi(1+\kappa)} \ln z_l \\
\chi_l'(z_l) &= \frac{\kappa(F_1 - iF_2)}{2\pi(1+\kappa)} \ln z_l
\end{aligned} \tag{12}$$

When either one of $F_i$, $i = 1,2$ is set to be 1, and the other is set to be 0, the fundamental solution where the concentrated force is applied in the direction of $x_i$, can be obtained using (12).

Then, one may ask, what is he relation between basis functions from different source points? Why T-Trefftz method cannot be used to solve problems in multiply connected domains with genus larger than 1, and why F-Trefftz method can be used for such a problem? Can we use multiple source points, as well basis functions of different orders, and how do we construct such a set of basis function? We answer these questions by analyzing the relation between basis functions from different source points using the binomial theorem and the logarithmic binomial theorem.

Consider two source points, and:

$$\begin{aligned} z_1 &= \left(x_1 - x_1^1\right) + i\left(x_2 - x_2^1\right) \\ z_2 &= \left(x_1 - x_1^2\right) + i\left(x_2 - x_2^2\right) \\ \Delta z &= z_2 - z_1 \end{aligned} \tag{13}$$

From the binomial theorem for positive power series, the second order case of which has been discovered by Greek Mathematician Euclid in as early as around 300 B.C., the higher order cases of which have been discovered by Yang Hui, Pascal and many others, we obtain:

$$z_2^n = (z_1 + \Delta z)^n = \sum_{k=0}^{n} \binom{n}{k} z_1^k \Delta z^{n-k}, \quad n \in \mathbf{Z}, \quad n \geq 0 \tag{14}$$

where the binomial coefficient is defined as:

$$\binom{n}{k} = \frac{n!}{k!\,(n-k)!}, \quad n,k \in \mathbf{Z}, \quad n \geq k \geq 0 \tag{15}$$

This binomial theorem was generalized by Isaac Newton in 1676 so that $n$ does not necessarily need to be positive. Applied to this particular problem, this generalized binomial theorem states:

$$\begin{aligned} z_2^n &= (z_1 + \Delta z)^n \\ &= \begin{cases} \sum\limits_{k=0}^{\infty} \binom{n}{k} z_1^k \Delta z^{n-k}, & |z_1| < |\Delta z| \\ \sum\limits_{k=0}^{\infty} \binom{n}{k} \Delta z^k z_1^{n-k}, & |z_1| > |\Delta z| \end{cases}, \quad n,k \in \mathbf{Z}, \quad n < 0, \quad k \geq 0 \end{aligned} \tag{16}$$

where the binomial coefficients were generalized to be:

$$\binom{n}{k} = \frac{n(n-1)...(n-k+1)}{k(k-1)...1}, \quad n,k \in \mathbf{Z}, \quad n < 0, \quad k \geq 0 \tag{17}$$

A further generalization, the so-called logarithmic binomial theorem, was derived in [Roman (1992)] by including some new functions called harmonic logarithms $\lambda_n^{(t)}(z)$, so that this algebra is close under both differentiation and anti-differentiation.

By taking $n = 0$ and $t = 1$, we have:

$$
\begin{aligned}
&\ln z_2 = \ln(z_1 + \Delta z) \\
&= \begin{cases}
\left\lfloor \begin{matrix} 0 \\ 0 \end{matrix} \right\rceil z_1^0 \ln \Delta z + \sum\limits_{k=1}^{\infty} \left\lfloor \begin{matrix} 0 \\ k \end{matrix} \right\rceil z_1^k \Delta z^{-k}, & |z_1| < |\Delta z| \\
\left\lfloor \begin{matrix} 0 \\ 0 \end{matrix} \right\rceil \Delta z^0 \ln z_1 + \sum\limits_{k=1}^{\infty} \left\lfloor \begin{matrix} 0 \\ k \end{matrix} \right\rceil \Delta z^k z_1^{-k}, & |z_1| > |\Delta z|
\end{cases}
\end{aligned}
\tag{18}
$$

where the binomial coefficients are generalized to be the so-called Roman coefficients:

$$
\begin{aligned}
&\left\lfloor \begin{bmatrix} n \\ k \end{bmatrix} \right\rceil = \frac{\lfloor n \rceil\,!}{\lfloor k \rceil\,!\,\lfloor n-k \rceil\,!}, \quad n,k \in \mathbf{Z} \\
&\lfloor k \rceil\,! = \begin{cases} n!, & n \in \mathbf{Z}, \quad n \geq 0 \\ \frac{(-1)^{-n-1}}{(-n-1)!}, & n \in \mathbf{Z}, \quad n < 0 \end{cases}
\end{aligned}
\tag{19}
$$

Based on the relations of Trefftz basis functions from different source points, we can draw the following important comments:

1. From (14), it is clear that a positive power function from one source point can be exactly expressed in terms of equal or less order positive power functions from an arbitrarily different source point. Therefore, one can only use positive power series from at most one source point as complex potentials, because otherwise the generated basis functions for the Trefftz method would not be linearly independent.

2. From (16) and (18), we can see that for a simply-connected domain which has a circular outer boundary, using only positive power function is complete. It can account for any possible singularities outside the outer boundary. If the outer boundary is not circular, such a conclusion cannot be made. However, based on previous study in the literature, it is generally found that if the outer boundary is piece-wise smooth, without notches or semi-circular cavities, and the traction distributed along the boundary is also piecewise-smooth, using only one source point with positive power complex potentials is good enough.

3. From (16) and (18), we can see that in order to reproduce a negative power function or a logarithmic function from one source point by functions from another source point, an infinite number of positive/negative power functions and a logarithmic function are needed as complex potentials. Therefore, using multiple negative power series and logarithmic functions from multiple source points as

complex potentials can be allowed in numerical implementation, where the linear independence of basis functions is preserved. Because complex potentials for fundamental solutions are in terms of logarithmic functions, as seen in (12), F-Trefftz method can use multiple source points.

4. From (16) and (18), we conclude that one should use at least negative power series and the logarithmic function from one source point in each cavity as complex potentials, in order for the set of constructed Trefftz basis functions to be complete. For example, as seen in Fig. 3, in order to reproduce $\ln z_2$ using Trefftz basis functions from source point $S_1$, only negative power series and logarithmic functions are needed for points where $|z_1| > |\Delta z|$, i.e. outside the dotted circle. On the other hand, for points where $|z_1| < |\Delta z|$, i.e. inside the dotted circle, only positive power series and the logarithmic function are needed. Therefore, it is impossible to reproduce $\ln z_2$ using positive/negative power series, and logarithmic function from source point $S_1$ in another cavity. For this reason, we conclude that at least one source point in each cavity should be selected where complex potentials are expressed in terms of negative power series and the logarithmic function.

5. From (16) and (18), we can see that for a circular cavity, putting one source point in the center of the cavity to account for the negative power and logarithmic complex potentials is sufficient. This is because the distance between the center of the circular and any other possible source point in the cavity, is smaller than the distance between the center of the circular cavity and any point of interest that is outside the circle.

6. For a cavity which is not circular-shaped, but have very simple geometry, using only one source point in this cavity can still be complete. However, this requires the technique of conformal mapping, as detailed demonstrated in the book of [Muskhelishvili (1954)]. By using conformal mapping $z_k = \omega(\varsigma_k)$, the $k^{th}$ cavity as in the space of $z_k$ is mapped into the space of $\varsigma_k$. The cavity appears to be circular-shaped in the space of $\varsigma_k$, so that the complex potentials can be expressed in terms of $\varsigma_k$, by using one source point in the center of the mapped circular cavity. Of particular interest are elliptical cavities, because the mapping rule is very simple.

7. For a cavity which has a complex geometry, a general polygon for example, using conformal mapping is complicated and inefficient. For this type of problems, it seems to be simpler to put multiple source points in the cavity in a similar manner of the F-Trefftz method, but one can still use multiple basis functions in each source point.

Based on these discussions, we propose a multi-source-point Trefftz method in section 3, and use a characteristic length for each point to scale the Trefftz basis functions, in order to resolve the ill-posedness of Trefftz methods.

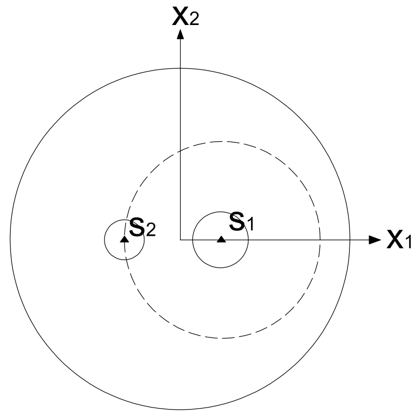


Figure 3: The relation between Trefftz basis functions from different source points

## 3 A Multi-Source-Point Multi-Characteristic-Length-Scale Trefftz Method

### 3.1 A Complete Set of Trefftz Basis Functions

In order to construct a complete set of Trefftz basis functions for arbitrarily multiply connected domain, we use multiple source points, and use two complex potentials for each source point. Several source points $S_k$ : $(x_1^k, x_2^k)$, $k = 1, 2...$, for negative power series and the logarithmic function are selected, so that each cavity should have at least one source point in it.

If the cavity is circular, only one source point is used, and is located in the center of the circle. At this source point, we have:

$$\begin{aligned} \phi_k(z_k) &= (iA_k + B_k)\ln z_k + \sum_{n=-1}^{-\infty} \left(i\alpha_{kn}^1 + \alpha_{kn}^2\right) z_k^n \\ \chi_k'(z_k) &= \kappa\,(iA_k - B_k)\ln z_k + \sum_{n=-1}^{-\infty} \left(i\alpha_{kn}^3 + \alpha_{kn}^4\right) z_k^n \end{aligned} \tag{20}$$

If the cavity is elliptical shaped with semi-axes $a_k, b_k$, we align the axes of local coordinate system $z_k$ to the axes of the ellipse, and use the simple conformal mapping

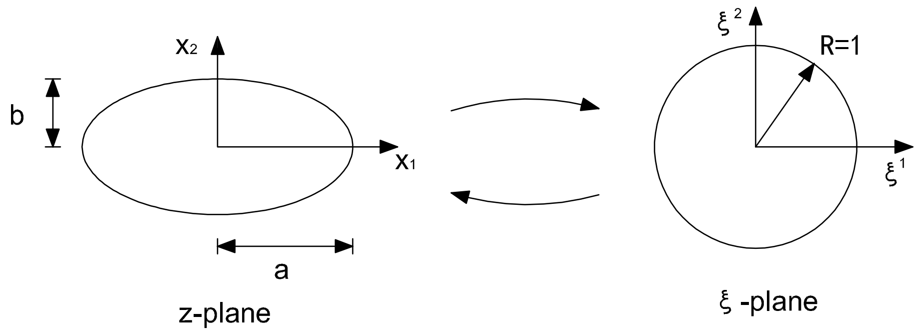


Figure 4: Conformal mapping from an ellipse to a unit circle

rule for ellipses, see Fig. 4:

$$\begin{aligned} z_k &= \omega_k(\varsigma_k) = c_k(\varsigma_k + \frac{m_k}{\varsigma_k}) \\ c_k &= \frac{a_k + b_k}{2} \\ m_k &= \frac{a_k - b_k}{a_k + b_k} \end{aligned} \tag{21}$$

And we have:

$$\varsigma_k = \omega^{-1}(z_k) = \frac{z_k \pm \sqrt{z_k^2 - 4c_k^2 m_k}}{2c_k} \tag{22}$$

The sign is determined by having a larger $|\varsigma_k|$.
At this source point, we have:

$$\begin{aligned} \phi_k(z_k(\varsigma_k)) &= (iA_k + B_k)\ln\varsigma_k + \sum_{n=-1}^{-\infty}\left(i\alpha_{kn}^1 + \alpha_{kn}^2\right)\varsigma_k^n \\ \chi_k'(z_k(\varsigma_k)) &= \kappa(iA_k - B_k)\ln\varsigma_k + \sum_{n=-1}^{-\infty}\left(i\alpha_{kn}^3 + \alpha_{kn}^4\right)\varsigma_k^n \end{aligned} \tag{23}$$

If the cavity is neither circular nor elliptical, instead of using complicated conformal mapping, we use multiple source points inside the cavity, and the complex potential in each source point is assumed in the form of (20).

Only one source point $S_p$ for positive power series are used, in order to preserve the linear independence of basis functions. And at this source point, we have non-singular complex potentials

$$
\begin{aligned}
\phi_p(z_p) &= \sum_{n=1}^{\infty} \left(i\alpha_{pn}^1 + \alpha_{pn}^2\right) z_p^n \\
\chi_p'(z_p) &= \sum_{n=0}^{\infty} \left(i\alpha_{pn}^3 + \alpha_{pn}^4\right) z_p^n
\end{aligned}
\tag{24}
$$

If there is only one elliptical cavity in the domain of interest, or if a simply connected elliptical domain is considered, it is natural to put the single source point $S_p$ at the center of the ellipse, and express the non-singular part of complex potentials as:

$$
\begin{aligned}
\phi_p(z_p(\varsigma_p)) &= \sum_{n=1}^{\infty} \left(i\alpha_{pn}^1 + \alpha_{pn}^2\right) \varsigma_p^n \\
\chi_p'(z_p(\varsigma_p)) &= \sum_{n=0}^{\infty} \left(i\alpha_{pn}^3 + \alpha_{pn}^4\right) \varsigma_p^n
\end{aligned}
\tag{25}
$$

In (25), if an elliptical hole is considered, the sign as in (22) is determined by having a larger $|\varsigma_p|$. If a simply-connected elliptical domain is considered, the sign is determined by having a smaller $|\varsigma_p|$.

### *3.2 Scaling the Trefftz Basis Functions by Characteristic Lengths*

As what is frequently encountered in Trefftz methods, if the basis functions described in section 3.1 is used, an ill-conditioned system of equations is to be solved in order to decide all the undetermined coefficients. This is because of the exponential growth of the term $z^n$ or $\varsigma^n$ with respect to the order $n$. [Liu (2007a, 2007b)] introduced the concept of using characteristic lengths to scale the Trefftz basis functions for Laplace equations. It is also applied in this study, in the context of linear elastic solid mechanics.

For each source point $S_k$ : $(x_1^k, x_2^k)$ in the form of (20), which is either the center of a circular cavity, or one of the multiple source points in a cavity with complicated geometry, a characteristic length $R_k$ is introduced, which should be the minimum distance in the space $z_k$ between the source point $S_k$ and any point where boundary conditions are specified, therefore $\left|\left(\frac{z_k}{R_k}\right)^n\right|$ is confined between 0 and 1 for any negative number $n$. Displacement fields from this source point are thereafter scaled as:

$$
\begin{aligned}
&u_1^k + iu_2^k = \left[\kappa\phi_k(z_k) - z_k\overline{\phi_k'(z_k)} - \overline{\chi_k'(z_k)}\right]/2G \\
&\quad \phi_k(z_k) = (iA_k + B_k)\ln\left(\frac{z_k}{R_k}\right) + \sum_{n=-1}^{-\infty}\left(i\alpha_{kn}^1 + \alpha_{kn}^2\right)\left(\frac{z_k}{R_k}\right)^n \\
&\quad \chi_k'(z_k) = \kappa(iA_k - B_k)\ln\left(\frac{z_k}{R_k}\right) + \sum_{n=-1}^{-\infty}\left(i\alpha_{kn}^3 + \alpha_{kn}^4\right)\left(\frac{z_k}{R_k}\right)^n
\end{aligned}
\tag{26}
$$

For each source point $S_k$ : $(x_1^k, x_2^k)$ in the form of (23), which is the center of an elliptical cavity, a characteristic length $R_k$ is also used. $R_k$ is defined as the maximum value which makes the following inequality holds for any point where the boundary conditions is prescribed:

$$
|\varsigma_k| = \omega^{-1}\left(\frac{z_k}{R_k}\right) \geq 1 \tag{27}
$$

Therefore $\left|\varsigma_k^n\right|$ is 0 and 1 for any negative $n$. If the boundary condition is prescribed along the elliptical hole, as in the direct problems, it is obvious that $R_k = 1$. The displacement field from this source point is:

$$
\begin{aligned}
u_1^k + iu_2^k &= \left[\kappa\phi_k(z_k(\varsigma_k)) - z_k\overline{\phi_k'(z_k(\varsigma_k))} - \overline{\chi_k'(z_k(\varsigma_k))}\right]/2G \\
&= \left[\kappa\phi_k(z_k(\varsigma_k)) - \frac{\omega_k(\varsigma_k)}{\overline{\dot{\omega}_k(\varsigma_k)}}\overline{\dot{\phi}_k(z_k(\varsigma_k))} - \overline{\chi_k'(z_k(\varsigma_k))}\right]/2G \\
\phi_k(z_k(\varsigma_k)) &= (iA_k + B_k)\ln\varsigma_k + \sum_{n=-1}^{-\infty}\left(i\alpha_{kn}^1 + \alpha_{kn}^2\right)\varsigma_k^n \\
\chi_k'(z_k(\varsigma_k)) &= \kappa(iA_k - B_k)\ln\varsigma_k + \sum_{n=-1}^{-\infty}\left(i\alpha_{kn}^3 + \alpha_{kn}^4\right)\varsigma_k^n
\end{aligned}
\tag{28}
$$

It should be noted that for an analytic function$f(z_k(\varsigma_k))$, $f'$ and $\dot{f}$ denote differentiation with respect to $z_k$ and $\varsigma_k$ respectively.

A characteristic length $R_p$ is also defined for the single source point $S_p$, which, on the contrary, should be the maximum distance between the source point $S_p$ and any point where boundary conditions are specified, therefore $\left|\left(\frac{z_p}{R_p}\right)^n\right|$ is confined between 0 and 1 for any positive $n$.Displacement fields from this source point are thereafter scaled as:

$$
\begin{aligned}
u_1^p + iu_2^p &= \left[\kappa\phi_p(z_p) - z_p\overline{\phi_p'(z_p)} - \overline{\chi_p'(z_p)}\right]/2G \\
\phi_p(z_p) &= \sum_{n=1}^{\infty}\left(i\alpha_{pn}^1 + \alpha_{pn}^2\right)\left(\frac{z_p}{R_p}\right)^n \\
\chi_p'(z_p) &= \sum_{n=0}^{\infty}\left(i\alpha_{pn}^3 + \alpha_{pn}^4\right)\left(\frac{z_p}{R_p}\right)^n
\end{aligned}
\tag{29}
$$

In a similar way, if (25) is used for the source point $S_p$, a characteristic length $R_p$ is used to scale the basis functions. $R_p$ is defined as the minimum value which makes the following inequality holds for any point where the boundary conditions is prescribed:

$$
|\varsigma_p| = \omega^{-1}\left(\frac{z_p}{R_p}\right) \leq 1 \tag{30}
$$

The displacement field from this source point is:

$$
\begin{aligned}
u_1^p + iu_2^p &= \left[\kappa\phi_p(z_p(\varsigma_p)) - \frac{\omega_p(\varsigma_p)}{\dot{\omega}_p(\varsigma_p)}\overline{\dot{\phi}_p(z_p(\varsigma_p))} - \overline{\chi_p'(z_p(\varsigma_p))}\right]/2G \\
\phi_p(z_p(\varsigma_p)) &= \sum_{n=1}^{\infty}\left(i\alpha_{pn}^1 + \alpha_{pn}^2\right)\varsigma_p^n \\
\chi_p'(z_p(\varsigma_p)) &= \sum_{n=0}^{\infty}\left(i\alpha_{pn}^3 + \alpha_{pn}^4\right)\varsigma_p^n
\end{aligned}
\tag{31}
$$

And the trial displacement field is a summation of contributions from all the source points:

$$
u_i = u_i^p + \sum_k u_i^k \tag{32}
$$

*This displacement assumption is generally valid for any multiply connected domain, and unknown coefficients can be determined by matching boundary conditions.*

*Here we define the inverse problem for elasticity as follows. If both the tractions as well as displacements are specified or known only on a part of the boundary, the problem is to determine the stresses and displacements in the domain as well as on the other part of the boundary. Likewise, if the strains can be measured instead of tractions, an equivalent problem may be to solve for the displacements and strains* *everywhere, when the strains as well as displacements are measured or specified only on a part of the boundary. In a multiply connected domain, the displacements and strains (or tractions) may be known or measured only at a part of the outer boundary, but such data is not available at the inaccessible cavities in the domain.*

In the next two sections, we develop Trefftz collocation methods for direct problems and for inverse Cauchy problems, respectively.

### 3.3 Trefftz Collocation Method for Direct Problems

Consider that $\overline{u}_i, \overline{t}_i$ are Cartesian components of the prescribed boundary displacement and boundary traction vector. $S_u, S_t$ are displacement boundary and traction boundary of the domain $\Omega$. The boundary conditions are:

$$\begin{aligned} u_i &= \overline{u}_i \text{ at } \mathrm{S}_u \\ n_j \sigma_{ij} &= \overline{t}_i \text{ at } \mathrm{S}_t \end{aligned} \tag{33}$$

If $S_u \cup S_t = \partial\Omega$, and $S_u \cap S_t = \emptyset$, it is considered as a direct problem. To be more specific, if $S_u = \partial\Omega, S_t = \emptyset$, it is a Dirichlet problem; if $S_t = \partial\Omega, S_u = \emptyset$, it is a Neumann problem; $S_u \neq \emptyset, S_t \neq \emptyset, S_u \cup S_t = \partial\Omega, S_u \cap S_t = \emptyset$, it is considered as a Robin problem. Otherwise, it is considered as an inverse problem.

Rewriting the trial functions as developed in section 3.2 in matrix/vector form, we have trial displacement field and its corresponding traction field as:

$$\begin{aligned} u_i(x_1,x_2) &= \mathbf{N}_i(x_1,x_2)\boldsymbol{\alpha} \\ t_i(x_1,x_2) &= \mathbf{R}_i(x_1,x_2)\boldsymbol{\alpha} \end{aligned} \tag{34}$$

$\boldsymbol{\alpha}$ contains all the undetermined coefficients $A_k, B_k, \alpha_{kn}^q, \alpha_{pn}^q,\ q = 1,2,3,4...$ These coefficients can be determined by any weighted-residual method: such as collocation, Galerkin method, the least squares method, or using boundary variational principle. In this study we simply collocate the displacement field at $P_u : (x_1^u, x_2^u) \in S_u$, u = 1,2,..., and collocate the traction field at $P_t : (x_1^t, x_2^t) \in S_t,\ t = 1,2,...$:

$$\begin{aligned} \mathbf{N}_i(x_1^u,x_2^u)\boldsymbol{\alpha} &= \bar{u}_i(x_1^u,x_2^u),\ u = 1,2... \\ w\mathbf{R}_i(x_1^t,x_2^t)\boldsymbol{\alpha} &= w\bar{t}_i(x_1^t,x_2^t),\ t = 1,2... \end{aligned} \tag{35}$$

or, in matrix/vector form:

$$\mathbf{A}\boldsymbol{\alpha} = \mathbf{b} \tag{36}$$

It should be noted that, in (35), a scalar $w$ is used as the weights for collocation equations of traction boundary conditions. This is to make the traction collocation equations have the same degree of importance as that of the displacement collocation equations. For the basis functions developed in section 3.2, it is obvious an appropriate choice of $w$ is $w = \frac{R_p}{2G}$.

For any finite multiply connected domain, if the resulted linearly independent collocation equations are more than the unknown coefficients, equations (36) can be solved in the sense of least squares. The unknown displacement, strain, stress and traction fields can thereafter be calculated.

However, for infinite domains, one needs also to match the remote stress field and rigid-body movements at infinity. For example, for an infinite body without rigid-body displacements under remote principal stress$N_1, N_2$, where the angle between axis $x_1$ and the direction of $N_1$ is $\alpha$, the boundary conditions at infinite location are satisfied by prescribing:

$$\begin{aligned} \phi_p(z_p) &= \frac{1}{4}(N_1+N_2)\,z_p \\ \chi_p'(z_p) &= -\frac{1}{2}e^{-2i\alpha}(N_1-N_2)\,z_p \end{aligned} \tag{37}$$

### *3.4 Trefftz Collocation Method with Regularization for Inverse Problems*

Strictly speaking, in an inverse Cauchy problem for plane elasticity, the tractions and displacements are prescribed or measured in part of $\partial\Omega$. However, in engineering applications, tractions are rarely measured. Strains can be easily measured instead. In this study, we considered two kinds of problems: (1) displacement and tractions, (2) displacements and strains are prescribed or measured at $S_C$, $S_C \subset \partial\Omega$. No information is given on the other part of $\partial\Omega$. Consider that $\overline{u}_i, \overline{t}_i, \overline{\varepsilon}_{ij}$ are Cartesian components of the prescribed boundary displacements, boundary tractions, and strains.

From the basis functions developed in section 3.2 and section 3.3, we have:

$$\begin{aligned} u_i(x_1,x_2) &= \mathbf{N}_i(x_1,x_2)\boldsymbol{\alpha} \\ t_i(x_1,x_2) &= \mathbf{R}_i(x_1,x_2)\boldsymbol{\alpha} \\ \varepsilon_{ij}(x_1,x_2) &= \mathbf{E}_{ij}(x_1,x_2)\boldsymbol{\alpha} \end{aligned} \tag{38}$$

For case (1), we have boundary conditions:

$$\begin{aligned} u_i &= \overline{u}_i \text{ at } \mathrm{S}_C \\ n_j\sigma_{ij} &= \overline{t}_i \text{ at } \mathrm{S}_C \end{aligned} \tag{39}$$

We collocate the displacements and tractions at points$P_k : (x_1^k, x_2^k) \in S_C$, k = 1,2,...,

$$\begin{aligned} \mathbf{N}_i(x_1^k,x_2^k)\boldsymbol{\alpha} &= \bar{u}_i(x_1^k,x_2^k),\ k=1,2... \\ w\mathbf{R}_i(x_1^k,x_2^k)\boldsymbol{\alpha} &= w\bar{t}_i(x_1^k,x_2^k),\ k=1,2... \end{aligned} \tag{40}$$

For this case, $w = \frac{R_p}{2G}$.
And for case (2) the boundary conditions are:

$$\begin{aligned} u_i &= \overline{u}_i \text{ at } S_C \\ \varepsilon_{ij} &= \bar{\varepsilon}_{ij} \text{ at } S_C \end{aligned} \tag{41}$$

We collocate the displacements and strains at points$P_k : (x_1^k, x_2^k) \in S_C$, k = 1,2,...,

$$\begin{aligned} \mathbf{N}_i(x_1^k, x_2^k)\boldsymbol{\alpha} &= \bar{u}_i(x_1^k, x_2^k),\ k = 1,2... \\ w\mathbf{E}_{ij}(x_1^k, x_2^k)\boldsymbol{\alpha} &= w\bar{\varepsilon}_{ij}(x_1^k, x_2^k),\ k = 1,2... \end{aligned} \tag{42}$$

For this case, $w = R_p$.
No matter for case (1) or (2), the resulting systems of equations can be rewritten in matrix/vector form:

$$\mathbf{A}\boldsymbol{\alpha} = \mathbf{b} \tag{43}$$

It is well-known that the inverse problems are ill-posed. A very small perturbation of the measurement data on the Cauchy boundary $S_C$, can lead to a significant change of the solution $u_i$ in the domain $\Omega$. For example, we can consider the problem of the doubly-connected domain in Fig. 1(b). The presence of the cavity allows the existence of singular basis function with the complex potential $z^{-m}, m > 0$. For a very large $m$, $z^{-m}$ decreases rapidly from the source point. Therefore, a large displacement field $u_i$ near the cavity with complex potentials $z^{-m}$ can lead to nearly no change to the displacement/traction/strain fields at the outer boundary. In other words, if the all the measurements are at the outer boundary, no information is given on the inner boundary, and the solutions are obtained by directly solve (43), a small perturbation of the measurement at the outer boundary will result in a large variation of the calculated displacement/strain/stress fields near the inner boundary.

In order to mitigate the ill-posedness of the inverse problem, regularization techniques can be used. For example, following the work of [Tikhonov and Arsenin (1977)], many regularization techniques were developed. [Hansen and O'Leary (1993)] has given an explanation that the Tikhonov regularization of ill-posed linear algebra equations is a trade-off between the size of the regularized solution, and the quality to fit the given data. With a positive regularization parameter $\gamma$, the solution is found by:

$$\min\left(\|\mathbf{A}\boldsymbol{\alpha} - \mathbf{b}\|_2^2 + \gamma\|\boldsymbol{\alpha}\|_2^2\right) \tag{44}$$

A fictitious time integration method was also developed by [Liu and Atluri (2009)], and its relation to filter theory was discussed. The solution is obtained by numerically integrating the systems of ordinary equations to a finite time $t$:

$$\dot{\boldsymbol{\alpha}} = -\mathbf{A}^{\mathbf{T}}\mathbf{A}\boldsymbol{\alpha} + \mathbf{A}^{\mathbf{T}}\mathbf{b} \tag{45}$$

However, it should be noted that these techniques are developed to solve the problem of discretized linear algebra equations $\mathbf{A}\boldsymbol{\alpha} = \mathbf{b}$, where $\mathbf{A}$ is an ill-conditioned matrix so that a small perturbation of $\mathbf{b}$ can lead to a large change of $\alpha$. But this is not the problem here, because as will be shown in section 4, matrix $\mathbf{A}$ is already made well-posed by scaling the Trefftz basis functions.

When displacements and tractions are specified on the partial boundary $S_C$, an appropriate regularization method is to find the solution by:

$$\min\left(\frac{\int_{S_C}(u_i-\bar{u}_i)^2\,dS}{\int_{S_C}dS}+\frac{\int_{S_C}(wt_i-w\bar{t}_i)^2\,dS}{\int_{S_C}dS}+\gamma\frac{\int_\Omega u_i^2\,d\Omega}{\int_\Omega d\Omega}\right) \tag{46}$$

Alternatively, if some uniformly distributed points $P_k : (x_1^k, x_2^k) \in S_C$, k = 1,2,...M, are selected, and some uniformly distributed points $P_l : (x_1^l, x_2^l) \in \Omega$, $l$ = 1,2,...N, are selected, a discretized version of (46) can be written as:

$$\min\left(\frac{\sum\limits_{k=1}^{M}\left(u_i^k-\bar{u}_i^k\right)^2}{M}+\frac{\sum\limits_{k=1}^{M}\left(wt_i^k-w\bar{t}_i^k\right)^2}{M}+\gamma\frac{\sum\limits_{l=1}^{N}\left(u_i^l\right)^2}{N}\right) \tag{47}$$

Consider that $\left\{u_1^l, u_2^l \,|\, l = 1,2...N\right\}^T = \mathbf{B}\boldsymbol{\alpha}$, then one can readily find that (47) is the same as:

$$\min\left(\frac{\|\mathbf{A}\boldsymbol{\alpha}-\mathbf{b}\|_2^2}{M}+\gamma\frac{\|\mathbf{B}\boldsymbol{\alpha}\|_2^2}{N}\right) \tag{48}$$

And (48) directly leads to the solution:

$$\boldsymbol{\alpha} = \left(\frac{\mathbf{A}^{\mathbf{T}}\mathbf{A}}{M}+\gamma\frac{\mathbf{B}^{\mathbf{T}}\mathbf{B}}{N}\right)^{-1}\frac{\mathbf{A}^{\mathbf{T}}\mathbf{b}}{M} \tag{49}$$

Similarly, when displacements and strains are measured on the partial boundary $S_C$, the same formulation as in (49) can be obtained.

## 4 Numerical Examples

In this section, numerical examples are conducted to validate our detailed discussions of the Trefftz basis functionsin section 2, and the performance of the proposed multiple-source-point Trefftz method in section 3. For all these examples, plane stress problems with $E = 1,\ v = 0.25$ are considered.

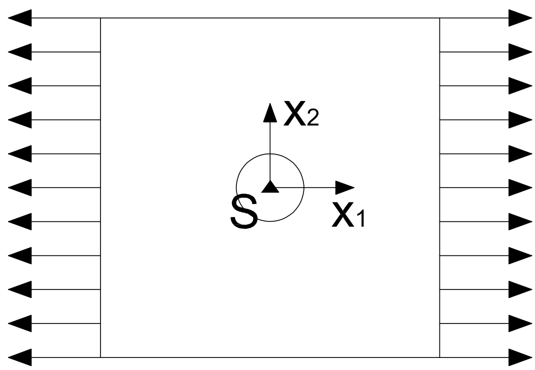


Figure 5: An infinite plate with a circular hole under remote tension

We consider the problem of an infinite plate with a circular hole as in Fig. 5 under remote tension. Exact solution of this problem can be found in [Muskhelishvili (1954)]. For a remote tension $T$ in positive $x_1$ direction, the complex potential for the exact solution can be expressed in $z$:

$$\begin{aligned} \phi(z) &= \frac{T}{4}(z + \frac{2R^2}{z}) \\ \chi'(z) &= -\frac{T}{2}(z + \frac{R^2}{z} - \frac{R^4}{z^3}) \end{aligned} \tag{50}$$

where $R$ is the radius of the circular hole.

Although this is actually a problem of doubly connected infinite domain, a truncated domain is used here instead. The displacement boundary condition is specified at the outer as well as the interior boundary by (50). A $100 \times 100$ square plate is considered, and the radius of the hole is taken to be 10. We locate the Trefftz source point at the center of the circular hole, and collocate $u_1, u_2$ at 40 uniformly distributed points at the outer boundary, and 40 more at the interior boundary.

We firstly illustrate why it is necessary to use characteristic lengths to scale Trefftz basis functions. In order to do this, this Dirichlet problem is solved with and without using characteristic lengths. When using characteristic lengths, $100\sqrt{2}$ is used for positive power series, and 10 is used for negative power series. Different numbers of Trefftz basis functions are used, but the positive and negative power series are kept to be complete to the same order. For example, when using 44 basis functions, power series are complete between the orders of -5 and 5. The condition numbers of computed coefficient matrix $\mathbf{A}$ as in (36) are plotted with respect to the numbers of basis functions used. As seen in Fig. 6, when using characteristic lengths to scale the Trefftz basis functions, the condition numbers are significantly reduced, and the ill-posedness of the Trefftz method is successfully resolved. Therefore, in the following numerical experiments, appropriate characteristic lengths are always used to scale the basis functions.

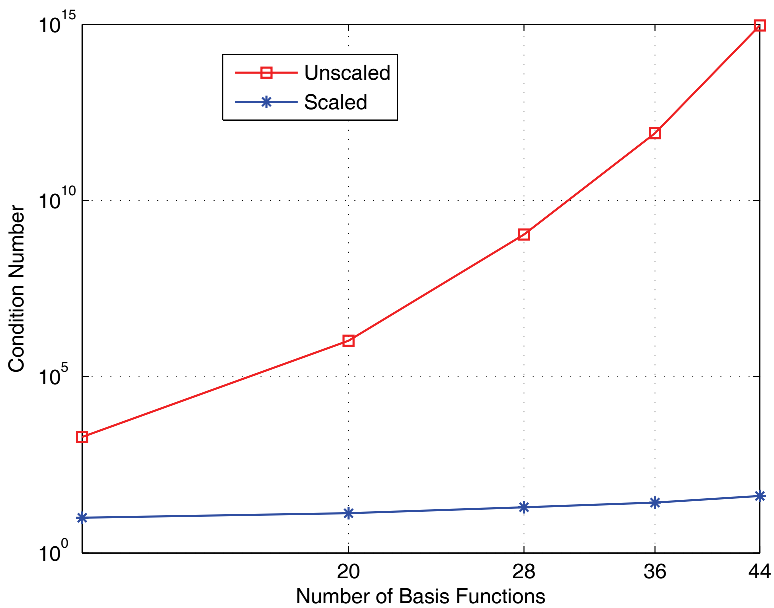


Figure 6: The condition number of the coefficient matrix with/without using characteristic lengths to scale Trefftz basis functions

We also use this problem to illustrate the importance of including negative power series as well as the logarithmic function as complex potentials. We firstly solve this problem by expressing the complex potentials only in terms of positive power series complete to the $8^{th}$ order. Then we solve this problem by using positive/negative power series between the order of -8 and 8, and the logarithmic function as complex potentials. The computed $\sigma_{11}$ and $\sigma_{22}$ are plotted along axis $x_2$ and $x_1$ respectively, in Fig. 7. As can be seen, by including negative power series and the logarithmic function, the solution is very accurate. However, by using only positive power series for this singular problem, the solution is much poorer. This is actually because of the singular nature of this stress concentration problem, which positive polynomial type of complex potentials cannot model. From this example, we can also gain some insights on why the Voronoi cell finite elements developed by [Ghosh, Lee and Moorthy (1995)] cannot successfully model the micromechanical behaviors of porous media, since the interior stress field of their elements is assumed as positive polynomial type of Airy stress functions.

We also consider the problem of an infinite plate with an elliptical hole as in Fig. 8 under remote tension. Exact solution of this problem can be found in [Muskhelishvili (1954)]. For a remote tension $T$ which has an intersection angle $\alpha$ with the positive $x_1$ axis , the complex potential for the exact solution can be expressed in $\varsigma$:

$$\begin{aligned} \phi(z(\varsigma)) &= \frac{Tc}{4}(\varsigma + \frac{2e^{2i\alpha}-m}{\varsigma}) \\ \chi'(z(\varsigma)) &= -\frac{Tc}{2}(e^{-2i\alpha}\varsigma + \frac{e^{2i\alpha}}{m\varsigma} - (1+m^2)\frac{(e^{2i\alpha}-m)}{m}\frac{\varsigma}{\varsigma^2-m}) \end{aligned} \tag{51}$$

where

$$\begin{aligned} z &= \omega(\varsigma) = c(\varsigma + \frac{m}{\varsigma}) \\ c &= \frac{a+b}{2} \\ m &= \frac{a-b}{a+b} \end{aligned} \tag{52}$$

$a,b$ are the length of semi-axes of the ellipse.

A $100 \times 100$ square plate is considered as the domain of interest, and $a,b$ is set to be 10 and 5 respectively. We consider a remote tension in the $x_2$ direction. We locate the Trefftz source point at the center of the elliptical hole, and collocate $u_1,u_2$ at 40 uniformly distributed points at the outer boundary, and collocate $t_1,t_2$ at 40 uniformly distributed points at the inner boundary.

We use this problem to illustrate the importance of conformal mapping for elliptical cavities. We firstly solve this problem by expressing the complex potentials in terms of $z$. Then we solve this problem by using conformal mapping, and expressing the complex potentials in terms of $\varsigma$. In each case, power series between the order of -8 and 8, and a logarithmic function, are used to construct Trefftz basis functions. The computed $\sigma_{11}$ and $\sigma_{22}$ are plotted along axis $x_2$ and $x_1$ respectively, in Fig. 9. As

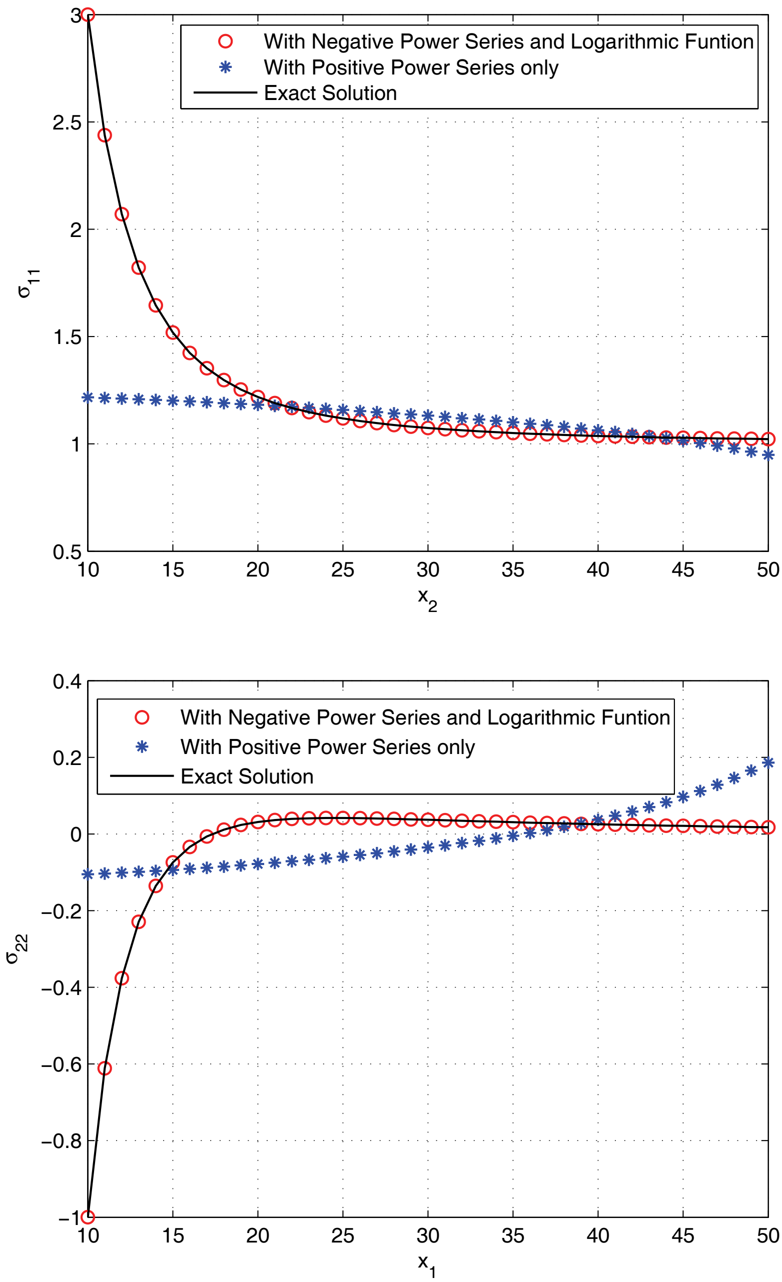


Figure 7: Computed $\sigma_{11}$ along axis $x_2$ , and computed $\sigma_{22}$ along axis $x_1$, with/without using negative power series and the logarithmic function as complex potentials

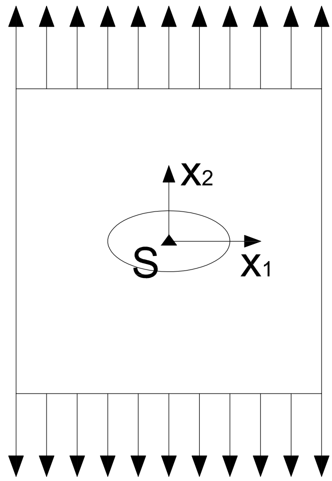


Figure 8: An infinite plate with an elliptical hole under remote tension

can be seen, by using conformal mapping, the solution is very accurate. However, without using conformal mapping, the solution is less satisfactory.

We also consider the problem of an infinite plate with a rectangular hole under remote tension, see Fig. 10. Theoretically speaking, exact solution of this problem requires conformal mapping which is infinite series:$z = \omega(\varsigma) = R(\frac{1}{\varsigma} + A\varsigma + B\varsigma^3 + C\varsigma^5 + ...)$, see [Savin (1961)]. However, keeping only the first four terms can produce a fairly reasonable result, as shown in [Lei, Ng, and Rigby (2001)]. In this study, we use the explicit result in [Lei, Ng, and Rigby (2001)] as the exact solution.

A $100 \times 100$ square plate is considered as the domain of interest, and both $a, b$ are set to be 20. We consider a remote tension in the $x_2$ direction. Collocations are conducted for $u_1, u_2$ at 80 uniformly distributed points at the outer boundary, and 80 more at the interior boundary.

We use this problem to illustrate the concept of using multiple source points in a complicated-shaped cavity. We firstly solve this problem by using one source point. In this case, power series between the order of -5 and 5, and a logarithmic function, are used to construct Trefftz basis functions. Then we solve this problem by using multiple source points. In this case, positive power series up to the order of 8 are used at only one source point—the center of the square. At the center point, logarithmic function and negative power series to the order -5 is used. At each one of the multiple source points near the inner boundary, only the logarithmic function

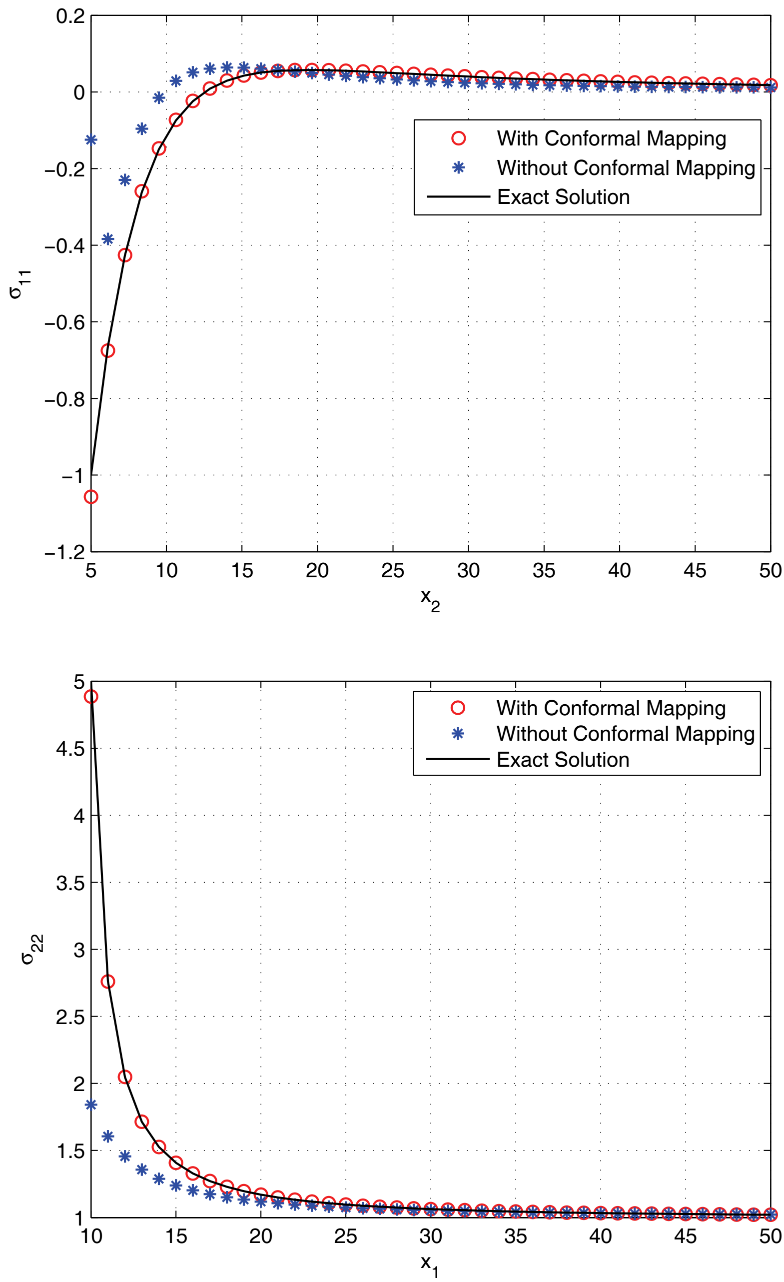


Figure 9: Computed $\sigma_{11}$ along axis $x_2$ , and computed $\sigma_{22}$ along axis $x_1$, with/without using conformal mapping

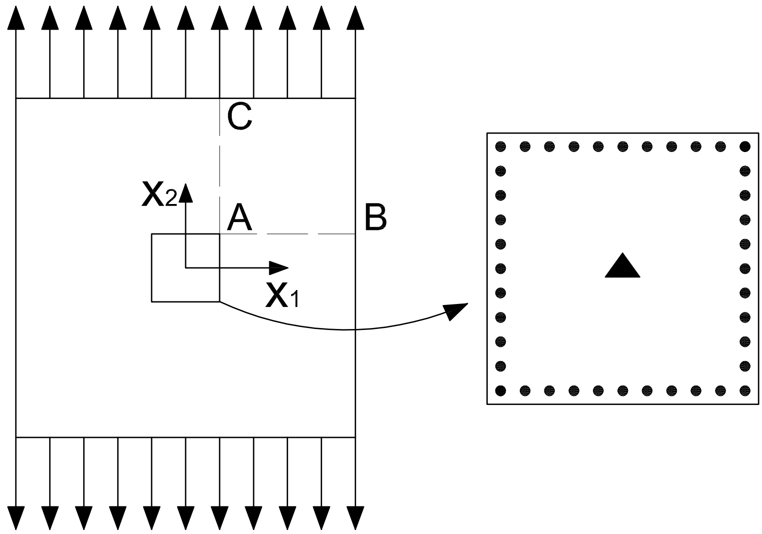


Figure 10: An infinite plate with a rectangular hole under remote tension, and the distribution of source points

and the function is used to construct the singular part of complex potential. The computed $\sigma_{11}$ and $\sigma_{22}$ are plotted along the line AA and the line BB, in Fig. 11(a) and Fig. 11(b). As can be seen, by using multiple source points, the accuracy is improved. If only one source point is used, the solution near the square is very poor, especially for $\sigma_{22}$.

In this example, we consider the problem of two unequal circular cavities in an infinite domain, under remote tension stress $T$, see Fig 12. The angle between the direction of axis $x_1$ and the direction of $T$ is $\alpha$. The radius of the two cavities are $R_1$ and $R_2$ respectively, and the distance of their centers is $d$. The analytical solution of this problem was found by [Haddon (1967)]. We consider the case of $T = 1$, $\alpha = \frac{\pi}{4}$, $R_1 = 1$, $R_2 = 2.5$, $d = 4.5$, and use multi-source-point as well as single-source-point Trefftz method to solve this problem. For multiple-source-point Trefftz method, the source points for negative power series and the logarithmic function are located at the two centers $S_1$ and $S_2$, and only $S_1$ is used for positive power series. For single-source-point Trefftz method, only source point $S_1$ is used. In both of the methods, power series between the order of $-20$ and 20, and the logarithmic function are used as complex potentials.

As discussed in section 3.3, for problems in an infinite domain, complex potentials $\phi_p, \chi_p'$ are determined beforehand, using (37). For this particular problem, obvi-

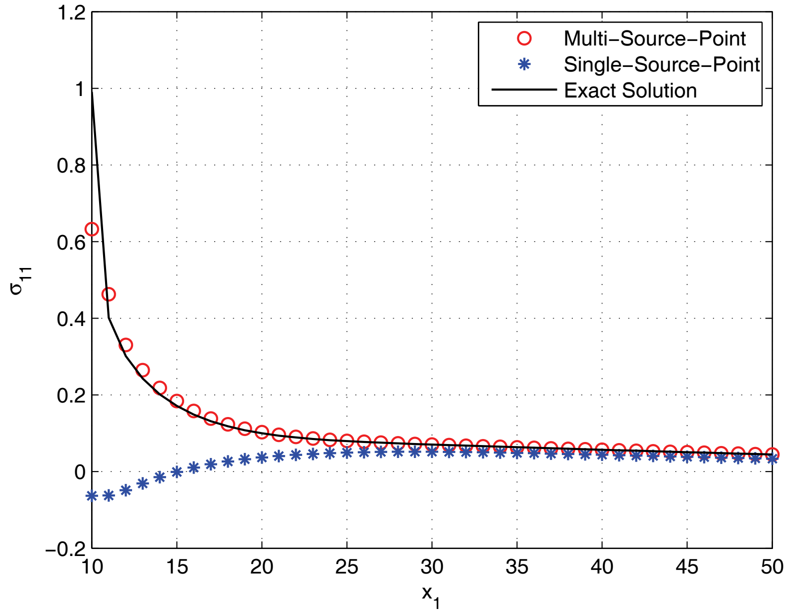


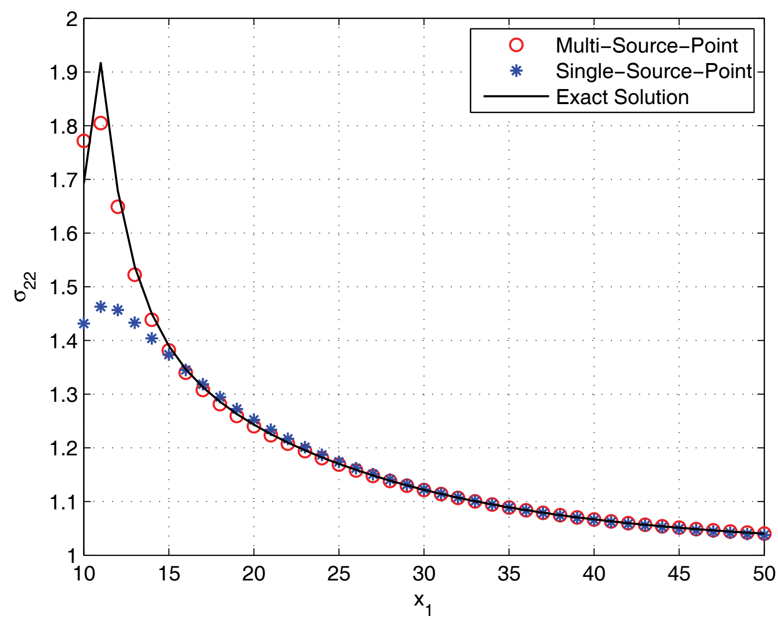


Figure 11(a): Computed $\sigma_{11}$ and computed $\sigma_{22}$ along the line AB, using a single source point and using multiple source points

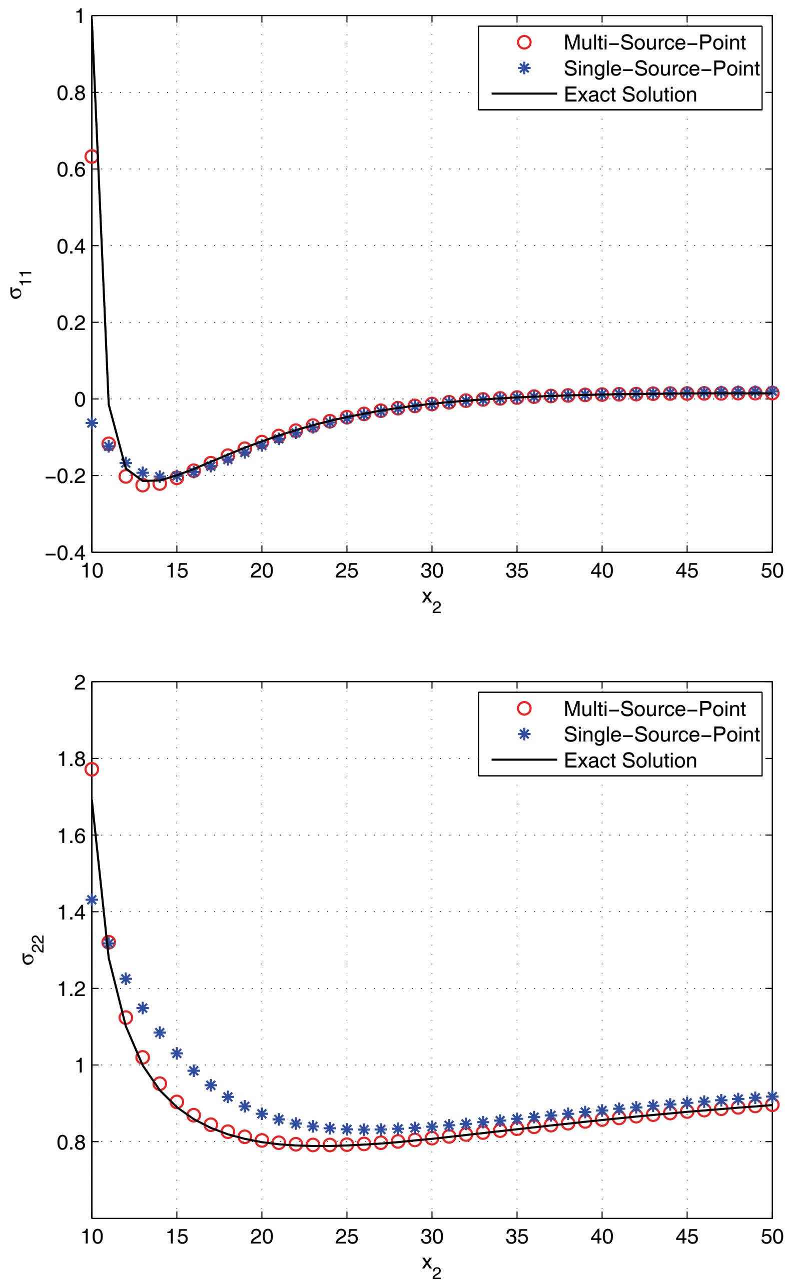


Figure 11(b): Computed $\sigma_{11}$ and computed $\sigma_{22}$ along the line AC, using a single source point and using multiple source points

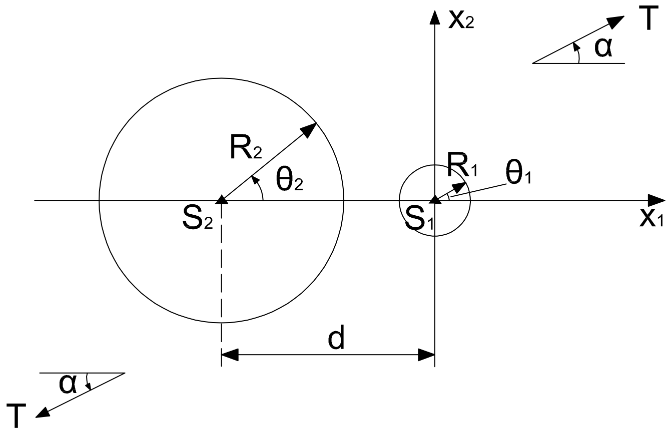


Figure 12: An infinite domain with two unequal circular cavities under remote tension

ously we have:

$$\begin{aligned} \phi_p(z_p) &= \frac{1}{4} T z_p \\ \chi_p'(z_p) &= -\frac{1}{2} e^{-2i\alpha} T z_p \end{aligned} \tag{53}$$

Coefficients of negative power series and logarithmic functions are determined by enforcing the traction-free condition at 48 uniformly distributed collocation points along each circle. The computed circumferential stresses $\sigma_{\theta\theta}$ along the boundary of the two circular cavities are shown in Tab. 1 and Tab. 2, and are plotted in 13 and Fig. 14. Compared to analytical solutions of [Haddon (1967)], we conclude that the multi-source-point Trefftz method can tackle this problem with very high accuracy, where the absolute error at any point is no larger than 0.001. On the other hand, the single-source-point Trefftz method failed to solve this problem. This is in agreement with our analysis in section 2:it is impossible to construct a complete set of Trefftz basis function using only one source point for a multiply connected domain with genus larger than 1.

*We also solve a Cauchy type of inverse problem.* A multiply connected domain is considered, see Fig 15. This domain is defined by three circles:

$$C1: \ (x_1-2)^2+(x_1-2)^2=1, \quad C2: \ (x_1+2)^2+(x_1+2)^2=1, \quad C3: \ x_1^2+x_2^2=16.$$

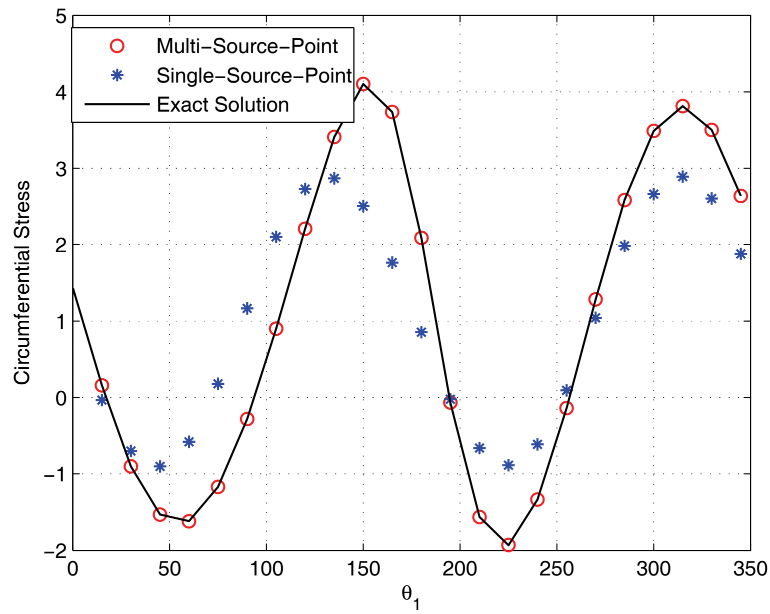


Figure 13: Circumferential stress $\sigma_{\theta\theta}$ with respect to $\theta_1$

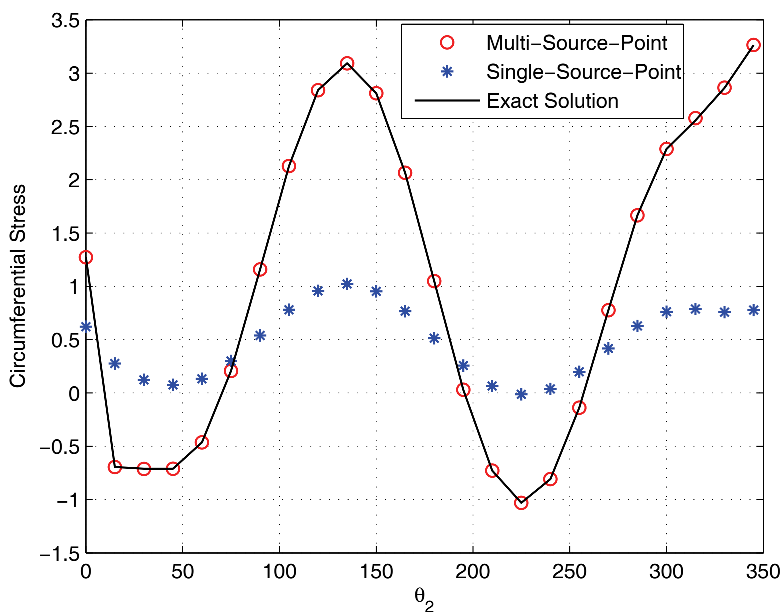


Figure 14: Circumferential stress $\sigma_{\theta\theta}$ with respect to $\theta_2$

Table 1: Computed circumferential stress $\sigma_{\theta\theta}$ along circle 1 using sing-source-point and multiple-source-point Trefftz method

| $\theta_1$(degree) | Single-Source-Point | Multi-Source-Point | Exact | $\theta_1$(degree) | Single-Source-Point | Multi-Source-Point | Exact |
|---|---|---|---|---|---|---|---|
| 0 | 0.912 | 1.432 | 1.432 | 180 | 0.855 | 2.089 | 2.089 |
| 15 | -0.034 | 0.159 | 0.159 | 195 | -0.021 | -0.067 | -0.067 |
| 30 | -0.700 | -0.902 | -0.902 | 210 | -0.662 | -1.563 | -1.563 |
| 45 | -0.901 | -1.531 | -1.531 | 225 | -0.884 | -1.932 | -1.932 |
| 60 | -0.579 | -1.618 | -1.618 | 240 | -0.612 | -1.335 | -1.335 |
| 75 | 0.180 | -1.170 | -1.170 | 255 | 0.0923 | -0.137 | -0.137 |
| 90 | 1.166 | -0.282 | -0.282 | 270 | 1.043 | 1.283 | 1.283 |
| 105 | 2.103 | 0.900 | 0.900 | 285 | 1.985 | 2.585 | 2.585 |
| 120 | 2.727 | 2.209 | 2.209 | 300 | 2.662 | 3.489 | 3.489 |
| 135 | 2.868 | 3.408 | 3.408 | 315 | 2.890 | 3.812 | 3.812 |
| 150 | 2.504 | 4.101 | 4.101 | 330 | 2.604 | 3.501 | 3.501 |
| 165 | 1.765 | 3.736 | 3.736 | 345 | 1.880 | 2.639 | 2.639 |

Table 2: Computed circumferential stress $\sigma_{\theta\theta}$ along circle 2 using sing-source-point and multiple-source-point Trefftz method

| $\theta_2$(degree) | Single-Source-Point | Multi-Source-Point | Exact | $\theta_2$(degree) | Single-Source-Point | Multi-Source-Point | Exact |
|---|---|---|---|---|---|---|---|
| 0 | 0.622 | 1.273 | 1.273 | 180 | 0.513 | 1.049 | 1.049 |
| 15 | 0.276 | -0.695 | -0.694 | 195 | 0.257 | 0.029 | 0.029 |
| 30 | 0.123 | -0.712 | -0.711 | 210 | 0.066 | -0.728 | -0.728 |
| 45 | 0.077 | -0.711 | -0.710 | 225 | -0.013 | -1.030 | -1.030 |
| 60 | 0.133 | -0.464 | -0.464 | 240 | 0.038 | -0.807 | -0.808 |
| 75 | 0.301 | 0.207 | 0.207 | 255 | 0.198 | -0.138 | -0.138 |
| 90 | 0.539 | 1.160 | 1.159 | 270 | 0.418 | 0.776 | 0.776 |
| 105 | 0.781 | 2.128 | 2.128 | 285 | 0.628 | 1.666 | 1.667 |
| 120 | 0.958 | 2.839 | 2.840 | 300 | 0.761 | 2.289 | 2.289 |
| 135 | 1.022 | 3.092 | 3.092 | 315 | 0.787 | 2.578 | 2.557 |
| 150 | 0.952 | 2.811 | 2.811 | 330 | 0.757 | 2.863 | 2.862 |
| 165 | 0.767 | 2.065 | 2.065 | 345 | 0.777 | 3.263 | 3.262 |

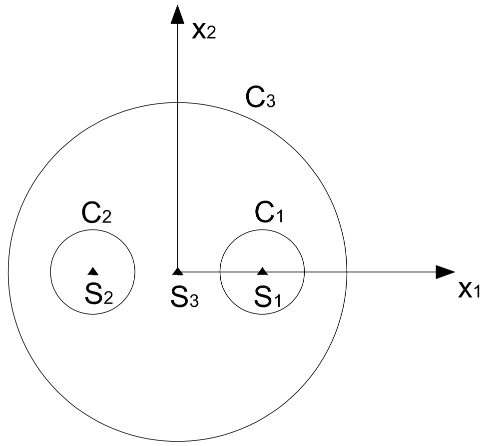


Figure 15: Solving a Cauchy type of inverse problem using multi-source-point Trefftz method

A solution which satisfies the governing differential equations is considered:

$$
\begin{aligned}
u_1 &= \frac{1}{2G}\left(\frac{\cos\theta_1}{r_1}+\frac{\cos 2\theta_2}{r_2^2}\right)\\
u_2 &= \frac{1}{2G}\left(\frac{\sin\theta_2}{r_1}+\frac{\sin 2\theta_2}{r_2^2}\right)
\end{aligned}
\tag{54}
$$

where $(r_1,\theta_1),(r_2,\theta_2)$ are polar coordinates with the centers of $C_1,C_2$ as origins respectively. Both displacement and traction boundary conditions are specified at the outer boundary $C_3$, but no information is given at the inner boundary $C_1,C_2$. This problem is to say: *if both the displacements and the tractions at the outer boundary are measured, can we identify the displacements specified or the tractions applied to the inner boundary, and of course, the displacement field in the whole domain?*

This problem is solved using multi-source-point Trefftz method. The source point for positive power series are located at $S_3$, the center of $C_3$, and the source points for negative power series and the logarithmic function are located at $S_1,S_2$ the centers of $C_1,C_2$ respectively. Positive power series are complete to the order of 5, negative power series are complete to the order of $-3$. Different levels of white noise are added to the measured displacements and tractions to test the robustness of this method. The regularization technique developed in section 3.4 is used, with regularization parameter$\gamma = 0.0001$.

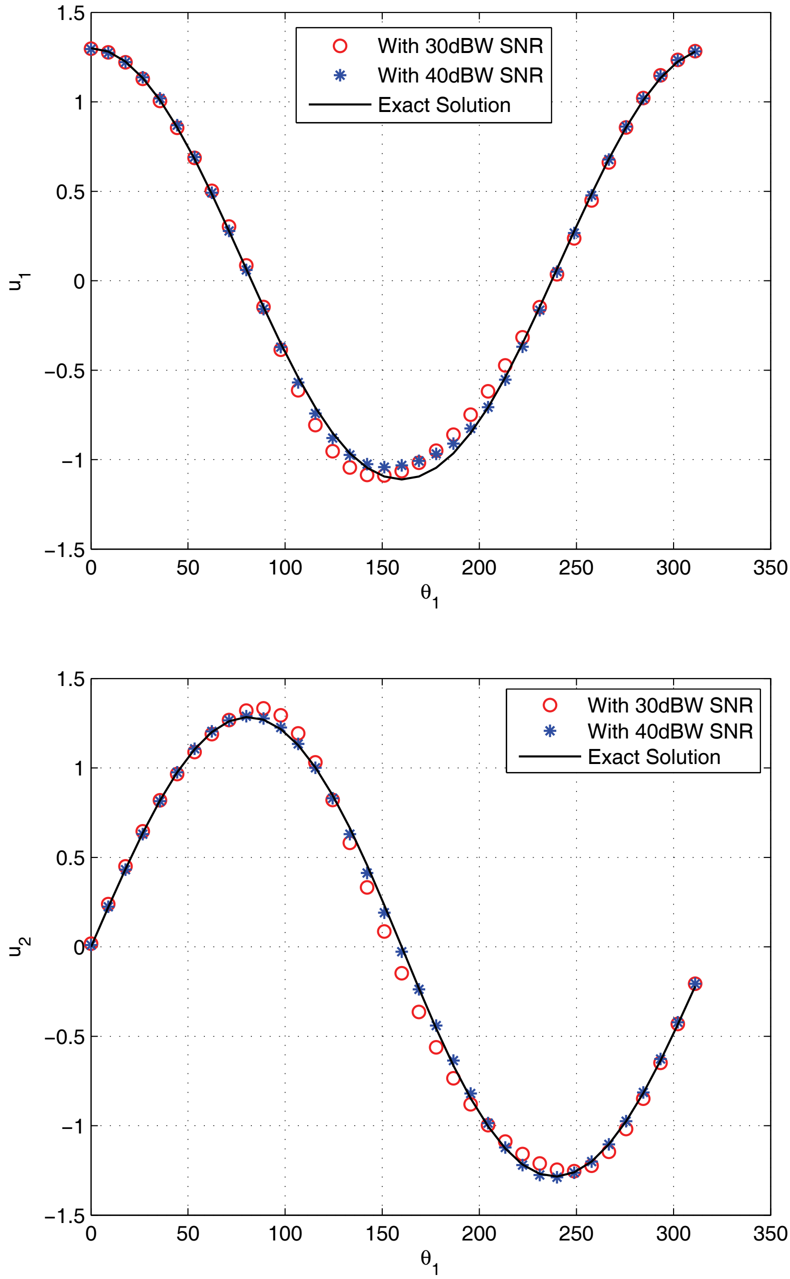


Figure 16: Comparison of the identified tractions $u_1$ and $u_2$ at $C_1$, with 30dBW/40dBW white noise added to the measured displacements and tractions at the outer boundary $C_3$

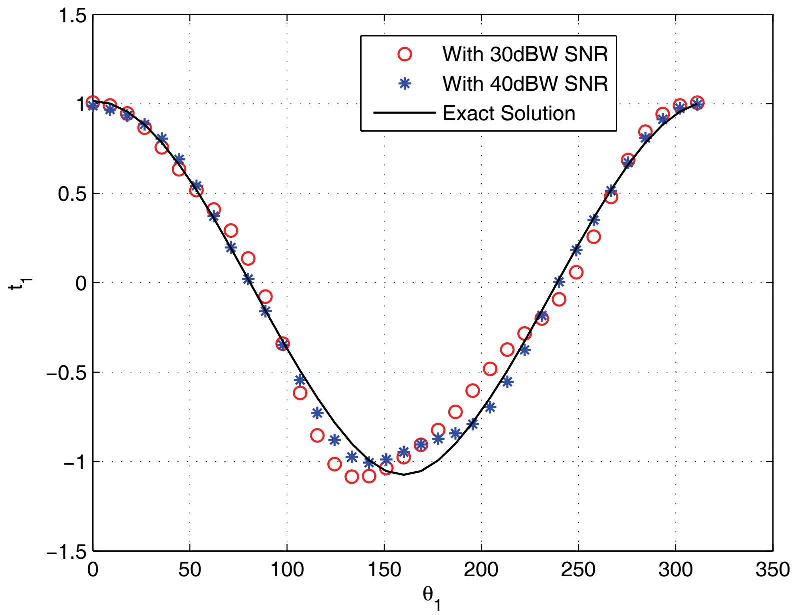


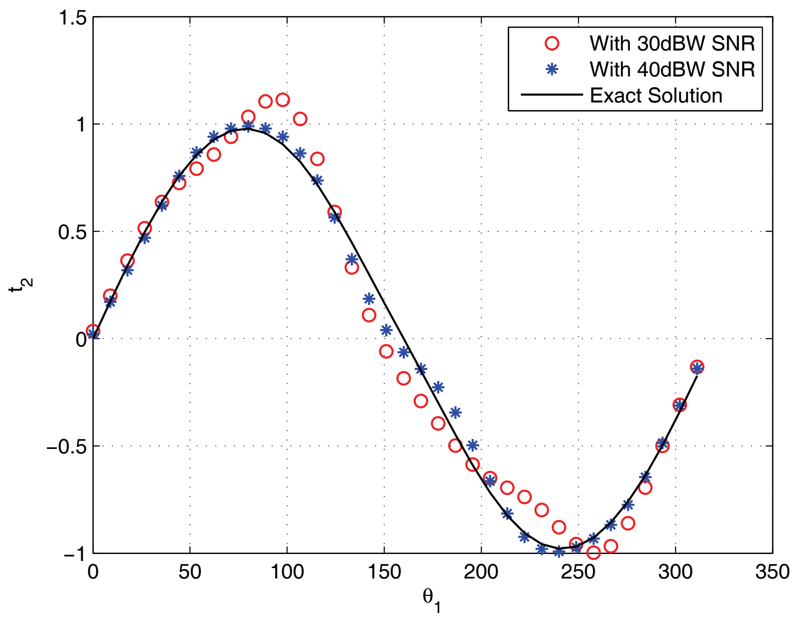


Figure 17: Comparison of the identified tractions $t_1$ and $t_2$ at $C_1$, with 30dBW/40dBW white noise added to the measured displacements and tractions at the outer boundary $C_3$

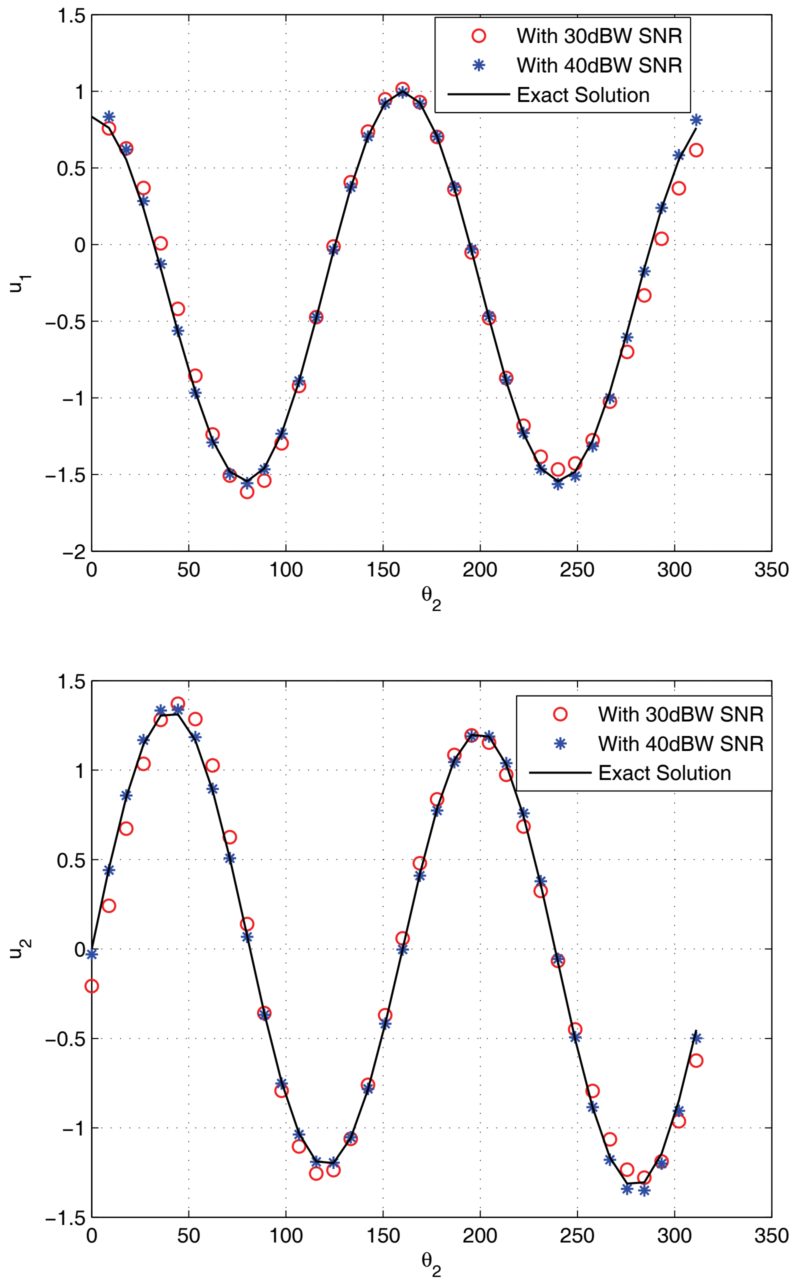


Figure 18: Comparison of the identified tractions $u_1$ and $u_2$at $C_2$, with 30dBW/40dBW white noise added to the measured displacements and tractions at the outer boundary $C_3$

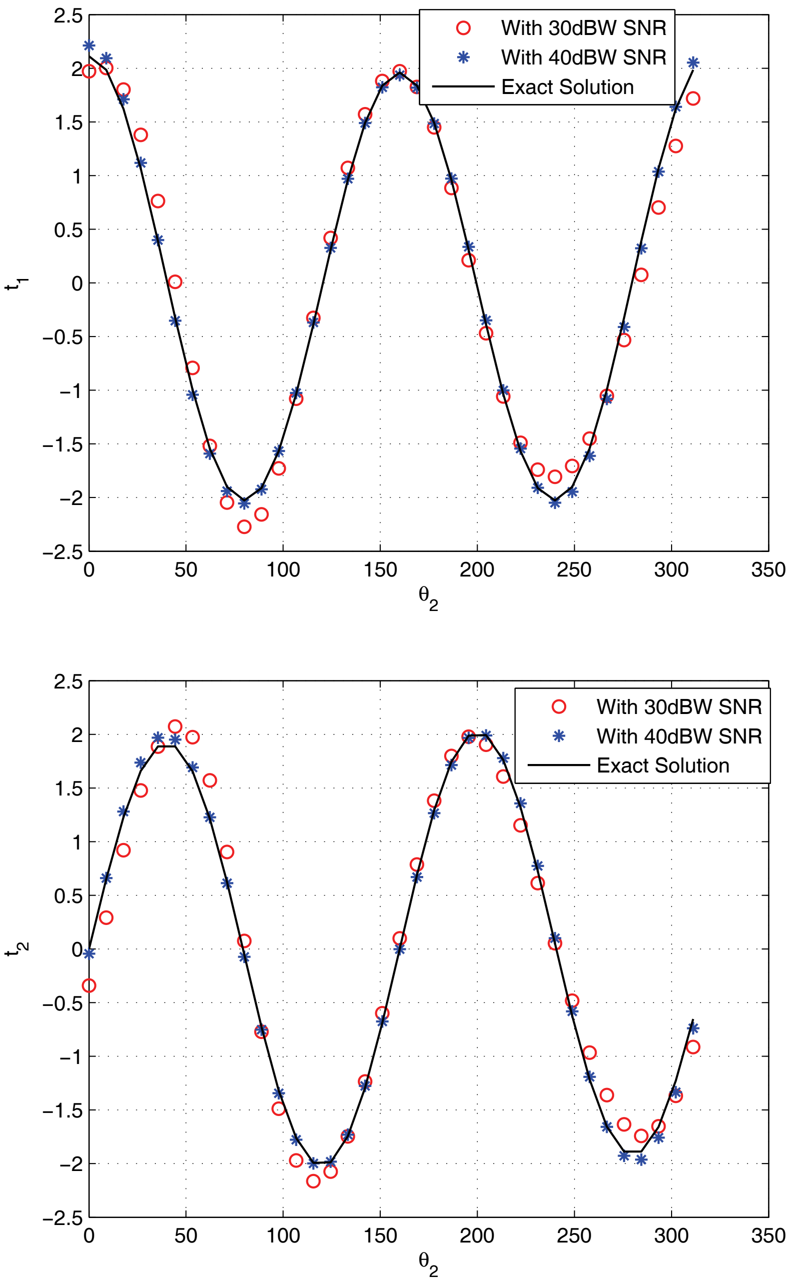


Figure 19: Comparison of the identified tractions $t_1$ and $t_2$at $C_2$, with 30dBW/40dBW white noise added to the measured displacements and tractions at the outer boundary $C_3$

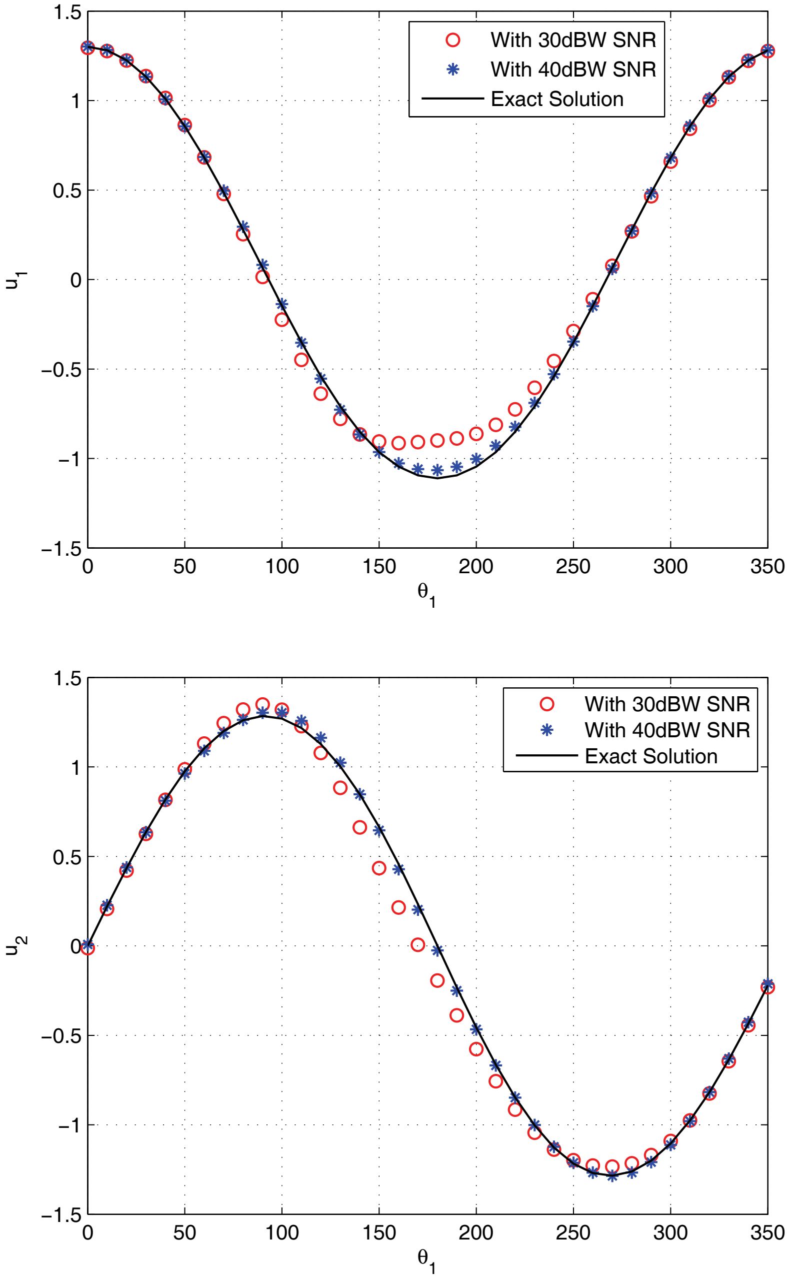


Figure 20: Comparison of the identified tractions $u_1$ and $u_2$ at $C_1$, with 30dBW/40dBW white noise added to the measured displacements and strains at the outer boundary $C_3$

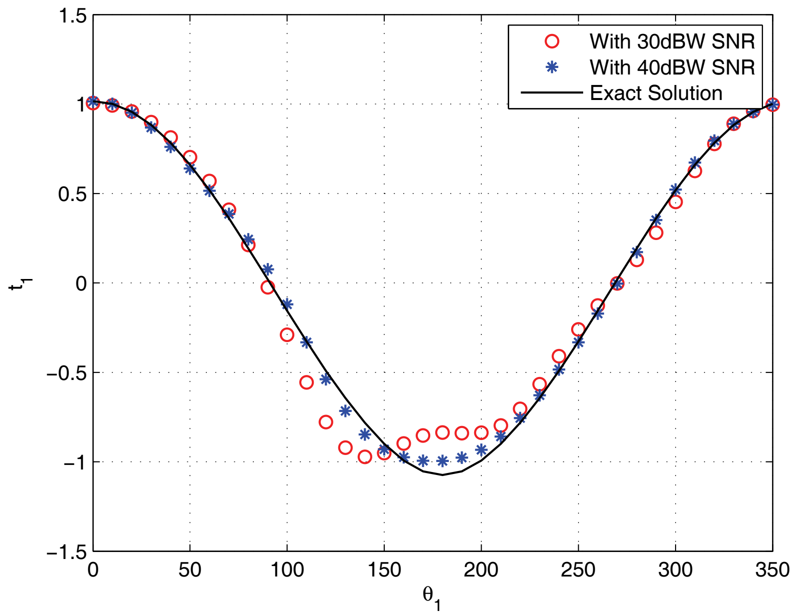


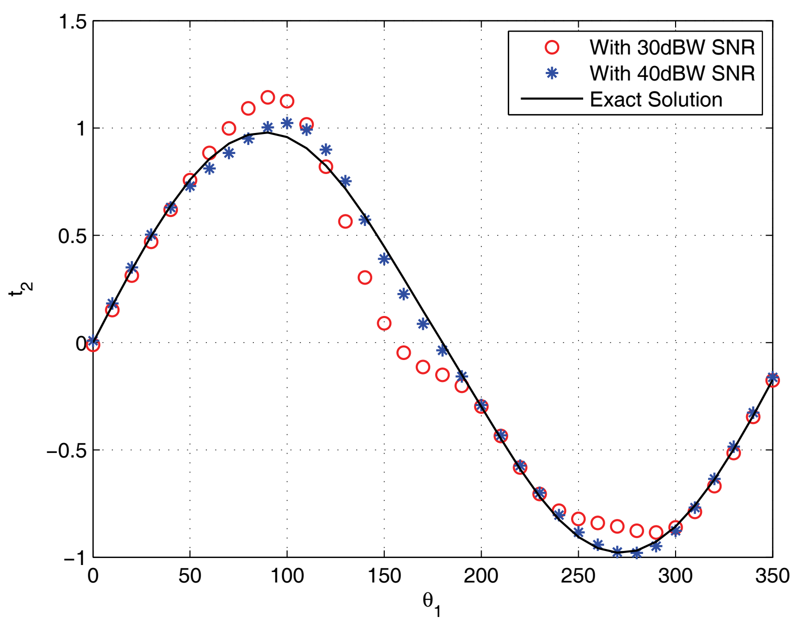


Figure 21: Comparison of the identified tractions $t_1$ and $t_2$at $C_1$, with 30dBW/40dBW white noise added to the measured displacements and strains at the outer boundary $C_3$

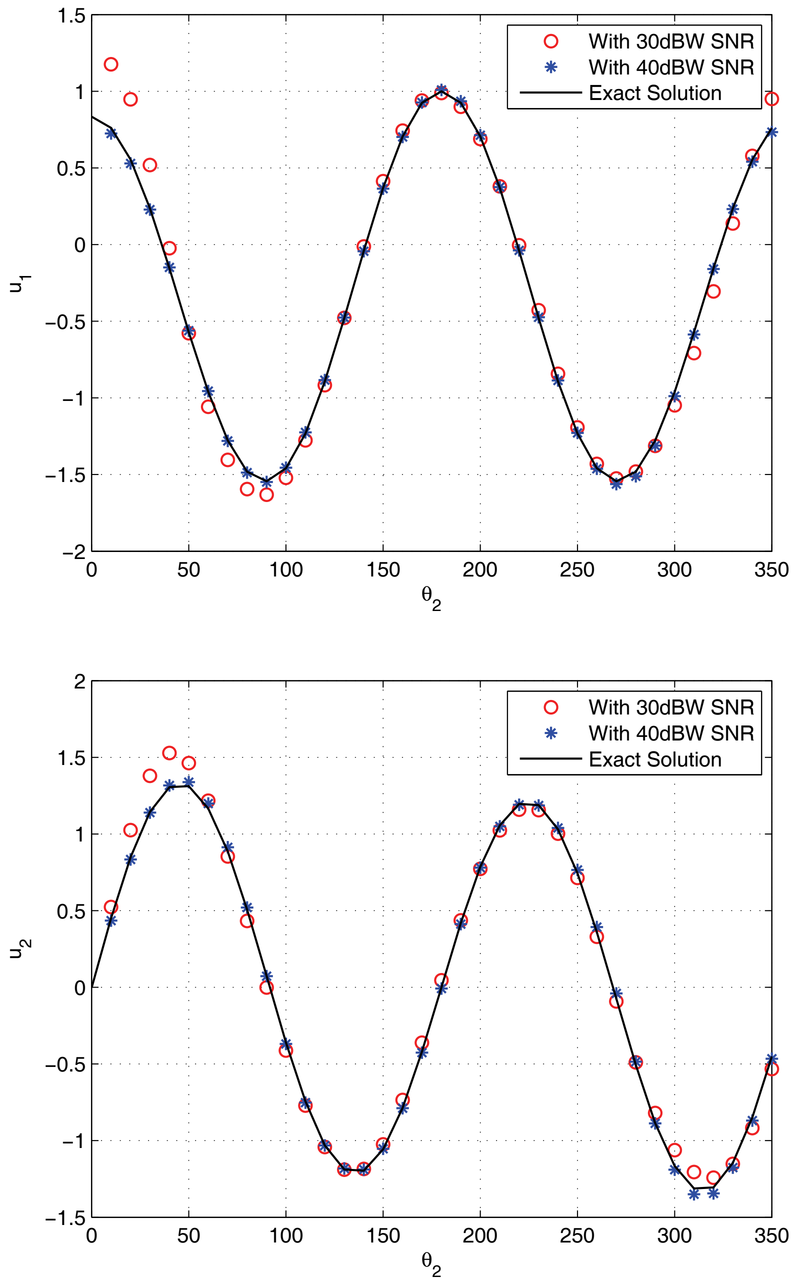


Figure 22: Comparison of the identified tractions $u_1$ and $u_2$at $C_2$, with 30dBW/40dBW white noise added to the measured displacements and strains at the outer boundary $C_3$

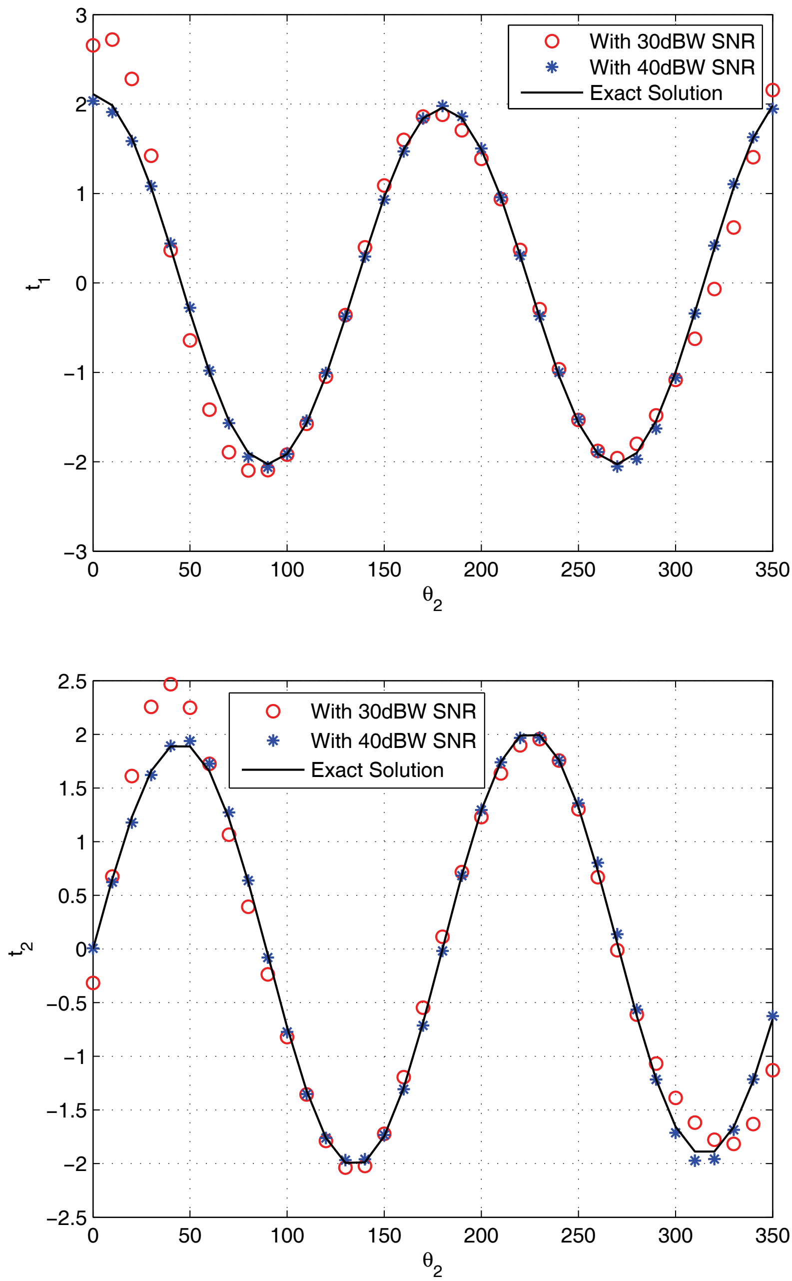


Figure 23: Comparison of the identified tractions $t_1$ and $t_2$ at $C_2$, with 30dBW/40dBW white noise added to the measured displacements and strains at the outer boundary $C_3$

Compared to (54), we find that when there is no noise present, this approach can always exactly reproduce the displacement field in the domain. When white noise with 30dBW and 40dBW signal to noise ratio (SNR) is added, or in other words, the amplitude of noise are 1% and 3.3% of the measurements, identified displacements and tractions at the inner boundary are compared with the exact tractions in Fig. 16-19. As can be seen, even with measurement noises, recovered fields are still of limited error.

In the last example, we solve the inverse problem again. *But at this time, the displacements and strains are measured at the outer boundary $C_3$, and no information is given at the inner boundaries.* Similarly, when no noise is present, the exact solution is reproduced. When white noise with 30dBW or 40dBW signal to noise ratio is added to the measured displacements and strains, identified displacements and tractions at the inner boundary are plotted in Fig. 20-23. Computed results are similar to that when displacements and tractions are specified.

## 5 Conclusion

A multi-source-point, multi-characteristic-length-scale, Trefftz method is developed, for solving direct/inverse problems of plane elasticity in multiply connected domains. Based on detailed discussion of the relations between Trefftz basis functions from different source points, simple rules on how to construct Trefftz basis functions from multiple source points are given, so that the constructed basis functions are complete for multiply connected domains. A characteristic length is also used for each source point to scale these basis functions, to avoid solving a system of ill-conditioned equations. For direct problems, no further regularization is needed. For inverse Cauchy problems where noise is present, a simple regularization method is used to mitigate the ill-posedness of the inverse problems. By several numerical examples, we clearly show that this method can efficiently and accurately solve both direct and inverse Cauchy problems in multiply connected domains. Therefore, we consider this unified approach to be simple, general as well as very useful, and the essential idea of how to construct basis functions from multiple source points can be used to develop other Trefftz methods, as well as special hybrid/mixed Trefftz finite elements.

We also point out that, although this method is developed in the context of two-dimensional linear elasticity, extension to three-dimensional problems will also be straight-forward, using the well-known Papkovich-Neuber solutions.

**Acknowledgement:** This work was supported in part by the Vehicle Technology Division of the Army Research Labs, under a collaborative research agreement with

University of California, Irvine (UCI), and in part by the Word Class University (WCU) program through the National Research Foundation of Korea, funded by the Ministry of Education, Science and Technology (Grant no.: R33-10049).

## References

**Chang, J. R.; Liu, R. F.; Kuo, S. R; Yeih, W.** (2003): Application of symmetric indirect Trefftz method to free vibration problems in 2D. *International Journal for Numerical Methods in Engineering*, vol. 56, issue 8, pp. 1175-1192.

**Cheung, Y. K.; Jin,W. G.; Zienkiewicz, O. C.** (1989): Direct solution procedure for solution of harmonic problems using complete, nonsingular, Trefftz functions. *International Journal for Communication in Applied Numerical Method*, vol. 5, issue 3, pp.159-169.

**Cheung, Y. K.; Jin,W. G.; Zienkiewicz, O. C.** (1990): Applications of the Trefftz method in plane elasticity problems. *International Journal for Numerical Methods in Engineering*, vol. 30, issue 6, pp.1147-1161.

**Cheung, Y. K.; Jin, W. G.; Zienkiewicz, O. C.** (1991): Solution of Helmholtz equation by Trefftz method. *International Journal for Numerical Methods in Engineering*, vol. 32, issue 1, pp.63-78.

**Cheung, Y. K.; Jin,W. G.; Zienkiewicz, O. C.** (1993): Trefftz method for Kirchhoff plate bending problems. *International Journal for Numerical Methods in Engineering*, vol. 36, issue 5, pp.765-781.

**Dong, L.; Atluri, S. N.** (2011): Development of T-Trefftz four-node quadrilateral and Voronoi Cell Finite Elements for macro- & micromechanical modeling of solids. *CMES: Computer Modeling in Engineering & Sciences*, vol.81, no. 1, pp.69-118.

**Dong, L.; Atluri, S. N.** (2012): T-Trefftz Voronoi Cell Finite Elements with Elastic/Rigid Inclusions or Voids for Micromechanical Analysis of Composite and Porous Materials. *CMES: Computer Modeling in Engineering & Sciences*, vol.83, no. 2, pp.183-220.

**Haddon, R. A. W**: Stresses in an infinite plate with two unequal circular holes. *The Quarterly Journal of Mechanics and Applied Mathematics*, vol. 20, issue 3, pp.277-291.

**Hansen, P. C.; O'Leary, D. P.** (1993): The use of the L-curve in the regularization of discrete ill-posed problems. *SIAM Journal of Scientific Computing*, vol. 14, pp. 1487-1503.

**Ghosh, S.; Lee, K.; Moorthy, S.** (1995): Multiple scale analysis of heterogeneous elastic structures using homogenization theory and Voronoi cell finite element method. *International Journal of Solids and Structures*, vol. 32, issue 1, pp. 27-63.

**Jirousek, J.; Teodorescu, P.** (1982): Large finite elements method for the solution of problems in the theory of elasticity. *Computers & Structures*, vol.15, issue 6, pp. 575-587.

**Jirousek, J.; Guex, Lan.** (1986): The hybrid-Trefftz finite element model and its application to plate bending. *International Journal for Numerical Methods in Engineering*, vol.23, issue 4, pp. 651-693.

**Kamiya, N.;Wu, S. T.** (1994): Genralized eigenvalue formulations of the Helmholtz equation by the Trefftz method. *Engineering Computations*, vol. 11, issue 2, pp. 177-186.

**Kita, E.; Kamiya, N.** (1995): Trefftz method: an overview. *Advances in Engineering Software*, vol. 24, issue 1-3, pp. 3-12.

**Kita, E.; Kamiya, N.; Iio, T.** (1999): Application of a direct Trefftz method with domain decomposition to 2D potential problems. *Engineering Analysis with Boundary Elements*, vol. 23, issue 7, pp. 539-548.

**Lei, C. M., Cherles, W. W. Ng., and Rigby, D. B.** (2001): Stress and displacement around an elastic artificial rectangular hole, *Journal of Engineering Mechanics*, vol. 127, No. 9, pp. 880–890.

**Li, Z. C.; Lu, T. T.; Tsai, H. S**.; Cheng, A. H. D. (2006): The Trefftz method for solving eigenvalue problems. *Engineering Analysis with Boundary Elements*, vol. 30, issue 4, pp. 292-308.

**Liu, C. S.** (2007a): A modified Trefftz method for two-dimensional Laplace equation considering the domain's characteristic length. *CMES: Computer Modeling in Engineering & Sciences*, vol.21, no. 1, pp.53-65.

**Liu, C. S.** (2007b): An effectively modified direct Trefftz method for 2D potential problems considering the domain's characteristic length. *Engineernig Analysis with Boundary Elements*, vol. 31, issue 12, pp. 983-993.

**Liu, C.-S.; Atluri, S. N.** (2009): A Fictitious time integration method for the numerical solution of the Fredholm integral equation and for numerical differentiation of noisy data, and its relation to the filter theory. *CMES: Computer Modeling in Engineering & Sciences*, vol. 41, pp. 243-261.

**Liu, C. S.; Yeih, W.; Atluri, S. N.** (2009): On solving the ill-conditioned system Ax=b: general-purpose conditioners obtained from the boundary-collocation solution of the Laplace equation, using Trefftz expansions with multiple length scales. *CMES: Computer Modeling in Engineering & Sciences*, vol. 44, no. 3, pp. 281-312.

**Muskhelishvili, N. I.** (1954): *Some Basic Problems of the Mathematical Theory of Elasticity*, $4^{th}$ edition, translated by Radok, Noordhoff, Leyden, The Netherlands, 1975.

**Roman, S.** (1992): The logarithmic binomial formula. *The American Mathematical Monthly*, vol. 99, no. 7, pp.641-648.

**Savin, G. N** (1961): *Stress Concentration around Holes*. Pergamon Press.

**Tikhonov, A. N.; Arsenin, V. Y.** (1977): *Solutions of Ill-Posed Problems*. John-Wiley & Sons, New York.

**Trefftz, E.** (1926): Ein Gegenstück zum Ritzschen Verfahren. *Proceedings of the second International Congress in Applied Mechanics*, Zurich, pp. 131-137.

**Yeih, W.; Liu, C. S.; Kuo, C. L.; Atluri, S. N.** (2010): On solving the direct/inverse Cauchy problems of Laplace equation in a multiply connected domain, using the generalized multiple-source-point boundary-collocation Trefftz method & characteristic lengths. *CMC: Computers, Materials & Continua*, vol. 17, no. 3, pp. 275-302.